

Mode-sum regularization of $\langle\phi^2\rangle$ in the angular-splitting method

Adam Levi and Amos Ori

*Department of physics,
Technion-Israel Institute of Technology,
Haifa 3200, Israel*

Abstract

The computation of the renormalized stress-energy tensor or $\langle\phi^2\rangle_{ren}$ in curved spacetime is a challenging task, at both the conceptual and technical levels. Recently we developed a new approach to compute such renormalized quantities in asymptotically-flat curved spacetimes, based on the point-splitting procedure. Our approach requires the spacetime to admit some symmetry. We already implemented this approach to compute $\langle\phi^2\rangle_{ren}$ in a stationary spacetime using *t-splitting*, namely splitting in the time-translation direction. Here we present the *angular-splitting* version of this approach, aimed for computing renormalized quantities in a general (possibly dynamical) spherically-symmetric spacetime. To illustrate how the angular-splitting method works, we use it here to compute $\langle\phi^2\rangle_{ren}$ for a quantum massless scalar field in Schwarzschild background, in various quantum states (Boulware, Unruh, and Hartle-Hawking states). We find excellent agreement with the results obtained from the *t-splitting* variant, and also with other methods. Our main goal in pursuing this new mode-sum approach was to enable the computation of the renormalized stress-energy tensor in a dynamical spherically symmetric background, e.g. an evaporating black hole. The angular-splitting variant presented here is most suitable to this purpose.

I. INTRODUCTION

The dynamical process of black-hole (BH) evaporation attracts much interest since Hawking’s discovery that BHs emit radiation [1]. This is because the BH evaporation phenomenon is intimately related to the connection between gravity and quantum mechanics. The main theoretical framework that allows us to study this process is semiclassical gravity. In this framework one considers a classical curved metric $g_{\alpha\beta}(x)$ with a quantum field. For simplicity we shall consider here a scalar field $\phi(x)$. This quantum field evolves according to Klein-Gordon equation

$$(\square - m^2 - \xi R)\phi = 0, \quad (1.1)$$

where m is the field’s mass¹ and ξ is its curvature coupling. The metric evolves according to the semiclassical Einstein equation

$$R_{\alpha\beta} - \frac{1}{2}Rg_{\alpha\beta} = 8\pi \langle T_{\alpha\beta} \rangle_{ren}, \quad (1.2)$$

where $R_{\alpha\beta}$ and R are the Ricci tensor and Ricci scalar, and $\langle T_{\alpha\beta} \rangle_{ren}$ is the renormalized expectation value of the stress-energy tensor of the quantum field. It is constructed from the fields’ modes, and it depends on the metric $g_{\alpha\beta}(x)$ (and on the field’s quantum state). Throughout this paper we use relativistic units $c = G = 1$.

All the above is known for four decades, and yet so far no one was able to solve these two coupled equations and provide detailed quantitative description of the semiclassical evaporation process. The main reason is that computation of the renormalized stress tensor turns out to be extremely difficult in a general curved background — even if the background metric $g_{\alpha\beta}(x)$ is prescribed. This difficulty emerges from the regularization process. Much like in flat spacetime, the “bare” expectation value of the stress tensor is divergent; nevertheless, in flat spacetime this divergence is easily handled using the *normal ordering* procedure. Unfortunately this simple procedure is not applicable in curved spacetime (mainly due to the non-existence of a unique time slicing).

In 1965 DeWitt developed a regularization method [2] for such divergent quantities named *point-splitting* or *covariant point separation*. DeWitt first illustrated the method for the regularization of $\langle \phi^2 \rangle$, and Christensen [3] later extended it to the stress-energy tensor. A key ingredient in this method is separating the evaluation point into a pair of nearby points x, x' and then taking the coincidence limit $x' \rightarrow x$ while subtracting some counterterm. This operation would presumably be feasible if the (modes of the) field $\phi(x)$ were known analytically. However, in BH backgrounds the field’s modes need to be computed numerically, and in such a case it becomes tremendously difficult to implement the above limiting procedure, at least in the direct naive way.

In the following years Candelas, Howard, Anderson and others developed procedures aimed for implementing the point-splitting method numerically, provided that one can compute the WKB approximation for the fields’ modes up to a sufficiently high order [4–7]. Alas, such computation of the WKB approximation is extremely difficult for a generic background. Even in the spherically-symmetric static case, the presence of a turning point makes the WKB expansion beyond leading order a very hard task — let alone the case of time-dependent background. For this reason most of these analyses were carried in the euclidian

¹ Throughout most of this paper, however, we shall consider the massless case $m = 0$.)

sector (which, however, is usually restricted to static situations). The most general case that was computed till recently was the spherically-symmetric static background, by Anderson [6] (for $\langle\phi^2\rangle$; and later on this computation was extended by Anderson, Hiscock and Samuel [7] to the renormalized stress-energy tensor). [8]

Recently we have developed a new approach for implementing the point-splitting procedure numerically, which does not rely on the WKB approximation at all (and can therefore be implemented directly in the Lorentzian sector). Instead, it only requires that the background admits some symmetry, which would allow mode decomposition of the field equation (like the spherical-harmonic or $e^{-i\omega t}$ decompositions in spherical or stationary backgrounds, respectively). The main idea behind our method is that, since the point-splitting counter term is known, one can decompose it and hence obtain from it “mode-wise” counter-terms that can be subtracted from the mode contributions, thereby regularizing their sum (or integral).

We developed several variants of this general method, which rely on different possible symmetries of the backgrounds in consideration. In the first paper [10] we have introduced the t -splitting variant which can be used in stationary backgrounds. To simplify things we have chosen (as usual) to first focus on the regularization of $\langle\phi^2\rangle$ rather than $\langle T_{\alpha\beta}\rangle$, as this quantity is less divergent and also it is a scalar, which significantly simplifies its presentation.

Even though the t -splitting variant is very efficient, as it can be used for every stationary background (e.g. a Kerr BH), it cannot be used to study dynamical processes, which is the most interesting case for us. In this paper we introduce the *angular-splitting* variant, which requires only spherical symmetry, and can be used in dynamical backgrounds. This paper, too, will focus on $\langle\phi^2\rangle$ for simplicity. In two forthcoming papers we shall present the extension of both the angular-splitting and t -splitting variants to the calculation of the renormalized stress-energy tensor.

The angular-splitting (or “ θ splitting”) variant is a bit more complicated than t -splitting. In principle, in this variant we aim to split the points in the θ direction, exploiting the spherical-harmonics decomposition. It turns out, however, that if the split is strictly in the angular direction we face an additional divergence in an intermediate stage (integration over the frequency ω). In order to cure this intermediate divergence we have to make an additional, smaller split ² in the t direction (see Sec. III). This slightly complicates the regularization procedure, but it’s worth it, because the resultant method is a very powerful one, being applicable to spherical dynamical backgrounds. In particular, it should be applicable to evaporating spherical BHs.

This paper is organized as follows: Section II briefly outlines the point-splitting procedure. In Sec. III we present the angular-splitting method for spherically-symmetric backgrounds, first in the static case and then also in the general time-dependent case. Section IV demonstrates the application of this method to the Schwarzschild case. We give the results for $\langle\phi^2\rangle_{ren}$ for a massless scalar field in the various vacuum states (Boulware, Unruh, and Hartle-Hawking). These results are compared with previous ones to find excellent agreement. Finally, in Sec. V we summarize and discuss our results.

² By “smaller split” we mean that we take this t -split to zero *before* taking the angular split to zero.

II. FIELD DECOMPOSITION AND BASIC POINT-SPLITTING PROCEDURE

A. Preliminaries

The angular splitting is designed to allow regularization in asymptotically flat, spherically-symmetric backgrounds, including time-dependent ones. We thus consider here the general double-null spherically-symmetric line element

$$ds^2 = -\Gamma(u, v) du dv + r^2(u, v) d\Omega^2 \quad (2.1)$$

(with $\Gamma > 0$), where $d\Omega^2 = d\theta^2 + \sin^2 \theta d\varphi^2$. It is also useful to define the corresponding space and time coordinates (t, z) via

$$v = t + z, \quad u = t - z,$$

in which the metric takes the form

$$ds^2 = \Gamma(t, z) (-dt^2 + dz^2) + r^2(t, z) d\Omega^2. \quad (2.2)$$

By virtue of asymptotic flatness, we set $\Gamma \rightarrow 1$ at spacelike infinity ($z \rightarrow \infty$).

In principle the coordinates u, v are subject to the gauge freedom $u \rightarrow u'(u), v \rightarrow v'(v)$. Employing asymptotic flatness we choose v to be an affine parameter along past null infinity (PNI). We leave the gauge of u unspecified for the time being, except that we assume that $u \rightarrow -\infty$ at PNI and (in case of a BH) $u \rightarrow \infty$ at the event horizon. In the static case, however, u is uniquely defined by the requirement of time-independent metric.

Owing to spherical symmetry of the background metric we can decompose the field in spherical harmonics Y_{lm} :

$$\phi(x) = \sum_{lm} c_{lm} Y_{lm}(\theta, \varphi) \Psi_l(t, z) / r, \quad (2.3)$$

where hereafter x denotes a spacetime point, and c_{lm} are arbitrary constants. The functions $\Psi_l(t, z)$ then satisfy the 2D field equation

$$\Psi_{l,uv} = -\frac{1}{4} V_l \Psi_l, \quad (2.4)$$

with the effective potential

$$V_l(u, v) = -4 \frac{r_{,uv}}{r} + \Gamma \left[\frac{l(l+1)}{r^2} + m^2 + \xi R \right], \quad (2.5)$$

where R is the Ricci scalar. For later convenience we also write the field equation using the t, z coordinates

$$\Psi_l'' - \ddot{\Psi}_l = V_l \Psi_l,$$

where henceforth dot and prime denote derivatives with respect to t and z respectively. In these coordinates the potential takes the form

$$V_l(t, z) = \frac{r'' - \ddot{r}}{r} + \Gamma \left[\frac{l(l+1)}{r^2} + m^2 + \xi R \right]. \quad (2.6)$$

The ω modes: From this point on we shall restrict our attention to the massless case $m = 0$. Owing to asymptotic flatness V_l vanishes at large r , hence at PNI Ψ_l asymptotically approaches some function of v , which we may denote as $\Psi_l^\infty(v)$.³

For concreteness we shall assume at this stage that the spacetime has a regular center (the case of eternal BH will be addressed later on). Then the initial function $\Psi_l^\infty(v)$ — along with the field equation (2.4) and the regularity condition

$$\Psi_l(t, r = 0) = 0 \quad (2.7)$$

at the center — uniquely determines the evolving solution $\Psi_l(t, z)$. The harmonic initial functions $\Psi_l^\infty(v) = e^{-i\omega v}$ play a key role in the theory, and we shall denote the functions $\Psi_l(t, z)$ which evolve from such harmonic PNI initial data by $\Psi_{\omega l}(t, z)$. Note that these functions depend on both ω (through initial conditions) and t . Using these ωl mode functions we can decompose the field as

$$\phi(x) = \sum_{lm} \int_0^\infty d\omega c_{\omega lm} f_{\omega lm}(x), \quad (2.8)$$

where $c_{\omega lm}$ are arbitrary expansion coefficients and

$$f_{\omega lm}(x) = Y_{lm}(\theta, \varphi) \bar{\Psi}_{\omega l}(t, z), \quad (2.9)$$

where

$$\bar{\Psi}_{\omega l}(t, z) \equiv \frac{\Psi_{\omega l}(t, z)}{r\sqrt{4\pi\omega}}. \quad (2.10)$$

The factor $1/\sqrt{4\pi\omega}$ was inserted in order for the $f_{\omega lm}$ modes to be properly Klein-Gordon normalized. Note that the $f_{\omega lm}$ functions satisfy the basic field equation (1.1) as well as the decomposed equation (2.4).

B. Quantum field:

The quantum field operator is constructed from the $f_{\omega lm}$ mode functions:

$$\phi(x) = \sum_{l=0}^{\infty} \int_0^\infty d\omega \sum_{m=-l}^l \left(f_{\omega lm}(x) a_{\omega lm} + f_{\omega lm}^*(x) a_{\omega lm}^\dagger \right), \quad (2.11)$$

where $a_{\omega lm}, a_{\omega lm}^\dagger$ are the creation and annihilation operators. We point out that one can choose different orders for the summation/integration operations. Here we choose the order which best suits our regularization procedure: Since we split in θ , the associated operation of summation over l should better be the last one. The order of ω -integration and m -summation is less crucial, however the one selected here is more convenient. Note that the field decomposition (2.11) naturally defines the *vacuum state* $|0\rangle$, which is annihilated by every $a_{\omega lm}$, namely $a_{\omega lm}|0\rangle = 0$ for every ωlm .

In the case of an eternal BH there is no regular center, instead there is a past horizon. One then has to introduce another set of modes defined with their own boundary conditions. This is addressed in Sec. III A 4 and III B (for the static and time-dependent cases, respectively).

³ To be more precise, the large- r asymptotic behavior of Ψ_l takes the form $\Psi_l^\infty(v) + \zeta_{\omega l}(u)$, where $\zeta_{\omega l}$ is some function of u . We refer to these two terms as the data at PNI and FNI respectively.

C. Calculation of $\langle \phi^2 \rangle_{ren}$

Trying to naively calculate the vacuum expectation value of ϕ^2 yields a divergent mode-sum

$$\langle \phi^2(x) \rangle_{naive} = \hbar \sum_{l=0}^{\infty} \int_0^{\infty} d\omega \sum_{m=-l}^l |Y_{lm}(\theta, \varphi)|^2 |\bar{\Psi}_{\omega l}(t, z)|^2. \quad (2.12)$$

As mentioned above one can consider different orders of summation and integration, yet they are all divergent. In the specific ordering (2.12) the sum over m converges of course (it is a finite sum), but the integral over ω diverges logarithmically. Furthermore, even after the divergence of the integral over ω is cured (as described below), the sum over l is also divergent, and even more strongly (like $l^2 \ln l$).

In the calculation of various renormalized quantities one often faces the situation in which an integral over ω fails to converge due to oscillations of the integrand at large ω . A similar problem of oscillations may also be faced in the summation over l (usually when the two points are separated in θ). To handle such non-convergent oscillations we employ the concept of *generalized integral* (or *generalized sum*), in which the oscillations are damped by multiplying the integrand (or sequence) by some factor exponentially-decaying in ω (or l) — and subsequently taking the limit of vanishing exponential pre-factor. This is described in more detail in Appendix A. We have already faced this problem of non-converging oscillatory integral over ω in our t -splitting variant. In Ref. [10] we explained the geometric origin of these large- ω oscillations (due to connecting null geodesics), and described their curing by generalized integration. We also prescribed our pragmatic method for implementing the generalized integral by *self-cancellation* of the oscillations. It is important to emphasize that all the sums and integrals in this paper are (at least in principle ⁴) *generalized* ones. Thus, by stating that the mode-sum in Eq. (2.12) diverges we actually mean it diverges even when the integral and sum are generalized.

Point splitting: In 1965 DeWitt showed [2] that one can consider the two-point function $\langle \phi(x) \phi(x') \rangle$, and obtain a meaningful (renormalized) expectation value of ϕ^2 by taking the coincidence limit

$$\langle \phi^2(x) \rangle_{ren} = \lim_{x' \rightarrow x} [\langle \phi(x) \phi(x') \rangle - G_{DS}(x, x')]. \quad (2.13)$$

Here $G_{DS}(x, x')$ is the DeWitt-Schwinger *counter-term*, a locally-constructed quantity which captures the singular piece of the two-point function at the limit $x' \rightarrow x$. For a scalar field with mass m ⁵ and coupling constant ξ it is

$$\frac{1}{\hbar} G_{DS}(x, x') = \frac{1}{8\pi^2 \sigma} + \frac{m^2 + (\xi - 1/6) R}{8\pi^2} \left[\gamma + \frac{1}{2} \ln \left(\frac{\mu^2 \sigma}{2} \right) \right] - \frac{m^2}{16\pi^2} + \frac{1}{96\pi^2} R_{\alpha\beta} \frac{\sigma^{;\alpha} \sigma^{;\beta}}{\sigma}, \quad (2.14)$$

where $R_{\alpha\beta}, R$ are the Ricci tensor and Ricci scalar, γ is Euler constant; and σ is the bi-scalar of the short geodesic connecting x to x' , which is equal to half the geodesic distance

⁴ Some of the integrals/sums in this paper do converge in the usual sense, but we are still allowed to regard them as generalized ones, for the following obvious reason: Whenever an integral/sum converges in the usual sense, it is guaranteed to coincide with the corresponding generalized integral/sum (see Appendix A).

⁵ Although this paper mainly addresses the massless case, for completeness we treat here the counter-term also in the $m \neq 0$ case.

squared (see Ref. [2]). The quantity μ is an unknown parameter, representing the well known ambiguity in the regularization process.

In the few cases that the modes are known analytically the recipe given by DeWitt can presumably be directly used to calculate $\langle \phi^2(x) \rangle_{ren}$, e.g. in the case of Robertson–Walker background [9]. However in most cases of interest, and particularly for BH backgrounds, the mode functions are known only numerically and with limited accuracy; namely $\bar{\Psi}_{\omega l}(t, z)$ is computed numerically for some finite range in ω , from zero to some ω_{max} (and for some range of $l \leq l_{max}$). Evaluation of the coincidence limit in Eq. (2.13) then becomes an extremely difficult task. As $x' \rightarrow x$ the ω_{max} and l_{max} values required for effective convergence grow rapidly, typically like the inverse of the separation.

Our approach of mode-sum regularization is tailored to overcome this difficulty: Essentially we handle the coincidence limit *analytically*, translating it to a certain regularization process which we implement while summing/integrating over the modes. Namely, we subtract certain functions of ω and l upon summation/integration. The entire numerical part of the calculation — the evaluation of the mode contributions and their sum/integral — is actually done *at coincidence*, which makes the entire numerical scheme tractable. We already described the application of this approach for t -splitting in Ref. [10]. Here we shall describe its application to θ -splitting.

III. THE ANGULAR-SPLITTING VARIANT

A. The static case

In order to make the regularization method more transparent we first present it for the special case of a static metric with a regular center (namely no eternal BH). In subsection III A 4 we describe the adjustment needed for an eternal BH background, and in Sec. III B we generalize it for dynamical backgrounds.

In the static case the general spherically-symmetric line element is

$$ds^2 = \Gamma(z) (-dt^2 + dz^2) + r^2(z) d\Omega^2. \quad (3.1)$$

The field is decomposed as in Eq. (2.9), but owing to time-translation symmetry the t dependence of $\bar{\Psi}_{\omega l}$ is now trivial:

$$\bar{\Psi}_{\omega l}(t, z) = e^{-i\omega t} \bar{\psi}_{\omega l}(z),$$

hence the mode decomposition becomes

$$f_{\omega l m}(x) = e^{-i\omega t} Y_{lm}(\theta, \varphi) \bar{\psi}_{\omega l}(z).$$

We again introduce the auxiliary function

$$\psi_{\omega l}(z) = r \sqrt{4\pi\omega} \bar{\psi}_{\omega l}(z) \quad (3.2)$$

which obeys the simple one-dimensional ODE

$$\psi''_{\omega l} = [V_l(z) - \omega^2] \psi_{\omega l}, \quad (3.3)$$

and the potential (2.6) now reduces to

$$V_l(z) = \frac{r''}{r} + \Gamma \left[\frac{l(l+1)}{r^2} + \xi R \right]. \quad (3.4)$$

(Recall that we restrict the analysis to massless fields.)

The boundary conditions for $\psi_{\omega l}$ are set such that the incoming monochromatic wave has a unit amplitude, and the modes are regular at the center. Owing to the presence of regular center, the reflected wave must have the same amplitude as the incoming one.⁶ Thus, the boundary conditions take the form

$$\psi_{\omega l}(r=0) = 0, \quad \lim_{z \rightarrow \infty} \psi_{\omega l}(z) = e^{-i\omega z} + e^{i\lambda(\omega, l)} e^{i\omega z}, \quad (3.5)$$

where $\lambda(\omega, l)$ is an unknown (real) phase associated to the reflected modes.

1. The integral over ω

The main essence of our regularization method is to split the points in a direction of symmetry, and to choose the order of the mode-sum operations such that the sum (or integral) that corresponds to the splitting direction is the last to be performed. Correspondingly, in the θ -splitting variant we perform the sum over l last. Thus, naively we would like to implement the point-splitting procedure in the following manner:

$$\langle \phi^2(x) \rangle_{split(naive)} = \lim_{\varepsilon \rightarrow 0} \left[\hbar \sum_{l=0}^{\infty} \int_0^{\infty} d\omega \sum_{m=-l}^l Y_{lm}(\theta, \varphi) Y_{lm}^*(\theta + \varepsilon, \varphi) |\bar{\psi}_{\omega l}(z)|^2 - G_{DS}(x, x') \right].$$

The sum over m is straightforward,

$$\sum_{m=-l}^l Y_{lm}(\theta, \varphi) Y_{lm}^*(\theta + \varepsilon, \varphi) = \frac{2l+1}{4\pi} P_l(\cos \varepsilon), \quad (3.6)$$

hence the first term in the squared brackets becomes

$$\hbar \sum_{l=0}^{\infty} \frac{2l+1}{4\pi} P_l(\cos \varepsilon) \int_0^{\infty} |\bar{\psi}_{\omega l}(z)|^2 d\omega.$$

It turns out, however, that the integral over ω still diverges. In fact, this integral is not affected at all by the splitting in θ , as one can easily verify.⁷ To see this divergence

⁶ This follows from the fact that at $r \rightarrow 0$ there exist, for any l , a regular solution ($\psi \propto r^{l+1}$) and a singular solution ($\psi \propto r^{-l}$). Since the radial equation is real, it immediately follows that the regular solution must be essentially real (namely, real, up to a constant pre-factor; otherwise, there would exist a second, independent, regular solution ψ^*). If the amplitudes of the outgoing and ingoing waves were different, the overall large- r asymptotic solution would fail to be (essentially) real.

⁷ Unlike what one might naively expect, certain mode-sum operations may diverge even when the points are separated. The convergence or otherwise of the mode-sum operations may depend on the splitting direction as well as on the order of these operations.

explicitly one can examine the large- ω asymptotic behavior of the modes. This large- ω analysis is presented in Appendix D (with fairly detailed description of the analysis in the case of static eternal BH, and summary of final results for the other, more complicated, cases). For a background with a regular center we obtain (see Sec. D 2 b)

$$|\bar{\psi}_{\omega l}(z)|^2 = \frac{1}{2\pi r^2 \omega} + (\dots), \quad (3.7)$$

where “(…)” denotes terms whose integral over ω converge. (Specifically it includes $\propto \omega^{-3}$ terms and also purely oscillatory terms whose amplitude decays as $1/\omega$.) Hence its integral over ω diverges logarithmically.

To overcome this divergence we introduce an additional splitting in the t direction, namely

$$x = (t, z, \theta, \varphi), \quad x' = (t + \delta, z, \theta + \varepsilon, \varphi).$$

However, this split in t is taken to be “small”, in the following sense: When implementing the coincidence limit we first take the limit $\delta \rightarrow 0$ and only afterwards the limit $\varepsilon \rightarrow 0$. Recalling Eq. (3.6), the renormalized vacuum expectation value of ϕ^2 now takes the form

$$\langle \phi^2(x) \rangle_{ren} = \lim_{\varepsilon \rightarrow 0} \lim_{\delta \rightarrow 0} \left[\hbar \sum_{l=0}^{\infty} \int_0^{\infty} d\omega \frac{2l+1}{4\pi} P_l(\cos \varepsilon) |\bar{\psi}_{\omega l}(z)|^2 e^{i\omega\delta} - G_{DS}(x, x') \right].$$

Since $G_{DS}(x, x')$ is regular even for $\delta = 0$ (as long as $\varepsilon > 0$), it is possible to rewrite this expression as

$$\langle \phi^2(x) \rangle_{ren} = \lim_{\varepsilon \rightarrow 0} \left[\lim_{\delta \rightarrow 0} \hbar \sum_{l=0}^{\infty} \frac{2l+1}{4\pi} P_l(\cos \varepsilon) \int_0^{\infty} |\bar{\psi}_{\omega l}(z)|^2 e^{i\omega\delta} d\omega - G_{DS}(\varepsilon) \right]. \quad (3.8)$$

Note the role of the two limits in this expression: The limit $\delta \rightarrow 0$ regulates the ω -integral, and subsequently the limit $\varepsilon \rightarrow 0$ controls the sum over l .

The counter-term G_{DS} is expressed in Eq. (2.14) as a function of the geodesic bi-scalar σ . Our calculation scheme requires us to re-express G_{DS} in terms of ε . In fact we find it most useful to expand G_{DS} in powers of $\sin(\varepsilon/2)$.⁸ To this end, in the first stage we expand the geodesic equation (integrated from θ to $\theta + \varepsilon$) to obtain σ Taylor-expanded in ε . This expansion is rather lengthy but is nevertheless straightforward, and it can be automated using standard algebraic-computation software. It yields

$$\sigma = \frac{r^2}{2} \varepsilon^2 + \tilde{c}(z) \varepsilon^4 + O(\varepsilon^5), \quad (3.9)$$

where

$$\tilde{c}(z) = -\frac{r^2}{24\Gamma} r'^2.$$

Then we re-expand it in $\sin(\varepsilon/2)$, and substitute in Eq. (2.14). We obtain the counter-term in the form

$$\frac{1}{\hbar} G_{DS}(\varepsilon) = a(z) \sin^{-2}(\varepsilon/2) + c(z) [\ln(\mu r \sin(\varepsilon/2)) + \gamma] + d(z) + O(\varepsilon), \quad (3.10)$$

⁸ This makes the Legendre decomposition (used below) simpler. Also in the Minkowski case, which provides a very useful guide, σ and G_{DS} are *exactly* proportional to $\sin^2(\varepsilon/2)$ and $\sin^{-2}(\varepsilon/2)$ respectively.

where $a(z), c(z), d(z)$ are coefficients that (in the massless case) take the form

$$\begin{aligned} a(z) &= \frac{1}{16\pi^2 r^2} , \\ c(z) &= \frac{(1/6 - \xi)}{8\pi^2 r^2 \Gamma^3} [-2\Gamma^3 - r^2 \Gamma'^2 + r^2 \Gamma \Gamma'' + 2\Gamma^2 r'^2 + 4r \Gamma^2 r''] , \\ d(z) &= -\frac{1}{48\pi^2 r \Gamma} r'' . \end{aligned}$$

The integral in Eq. (3.8) is regularized by the oscillating factor $e^{i\omega\delta}$, which provides an effective cutoff at $\omega \sim 1/\delta$. In order to regularize this integral at the $\delta \rightarrow 0$ limit, we next process this integral by the usual technique of adding and subtracting some ω -dependent quantity, which depicts the large- ω leading order of the integrand. (A successful subtraction of the divergent piece will eventually enable us to take the limit $\delta \rightarrow 0$ already in the integrand.) Utilizing the fact that the divergent piece in Eq. (3.7) is independent of l , we found that a convenient way to regularize the $\delta \rightarrow 0$ limit is to add and subtract the corresponding contribution from the $l = 0$ mode. Namely we write the integral in Eq. (3.8) as the sum of two integrals:

$$\int_0^\infty E_{\omega l} e^{i\omega\delta} d\omega = \int_0^\infty [E_{\omega l} - E_{\omega, l=0}] e^{i\omega\delta} d\omega + \int_0^\infty E_{\omega, l=0} e^{i\omega\delta} d\omega , \quad (3.11)$$

where for brevity we have defined

$$E_{\omega l}(z) \equiv |\bar{\psi}_{\omega l}(z)|^2 , \quad (3.12)$$

which represents the integrand at the coincide ($\delta = 0$). The first integral in the right-hand side now converges even for $\delta = 0$, so it is possible to take the limit by setting $\delta = 0$ already in the integrand.⁹ For brevity we denote this integral (with the limit $\delta \rightarrow 0$ already taken) by

$$F(l) \equiv \int_0^\infty [E_{\omega l} - E_{\omega, l=0}] d\omega . \quad (3.13)$$

This quantity can be computed directly once the modes $\bar{\psi}_{\omega l}(r)$ are known (even numerically). Note that $F(l)$ (like $E_{\omega l}$ and G_{DS} , and like Z below) depends on z as well. We often omit this z -dependence for brevity, although below we occasionally denote it as $F(l, z)$ when appropriate.

The second integral in Eq. (3.11) is more interesting, and we denote it as

$$Z(\delta) \equiv \int_0^\infty E_{\omega, l=0} e^{i\omega\delta} d\omega .$$

It is a well defined function of δ that diverges as $\delta \rightarrow 0$ (but finite otherwise). Note that $Z(\delta)$ also depends on z , but it does *not* depend on l .

⁹ This involves interchanging the order of the $\delta \rightarrow 0$ limit with the sum over l and the integral over ω . Although the mathematical justification of such an interchange is far from obvious, we find strong evidence for its validity from the asymptotic behavior of the various quantities at large ω and l . Other interchanges of operations are also used in a few other occasions later on. This issue is further discussed in Sec. V.

Substituting the ω -integral in (3.11) [which is now represented by $F(l) + Z(\delta)$] back in Eq. (3.8) yields

$$\langle \phi^2(x) \rangle_{ren} = \lim_{\varepsilon \rightarrow 0} \left[\hbar \sum_{l=0}^{\infty} \frac{2l+1}{4\pi} P_l(\cos \varepsilon) F(l) + \hbar \lim_{\delta \rightarrow 0} \left\{ \sum_{l=0}^{\infty} \frac{2l+1}{4\pi} P_l(\cos \varepsilon) Z(\delta) \right\} - G_{DS}(\varepsilon) \right]. \quad (3.14)$$

A crucial observation is that for any (small) ¹⁰ finite ε the term in curly brackets actually *vanishes*, because

$$\sum_{l=0}^{\infty} (2l+1) P_l(\cos \varepsilon) = 0.$$

This is shown in Appendix B. Equation (3.14) thus takes the simpler form

$$\langle \phi^2(x) \rangle_{ren} = \lim_{\varepsilon \rightarrow 0} \left[\hbar \sum_{l=0}^{\infty} \frac{2l+1}{4\pi} P_l(\cos \varepsilon) F(l) - G_{DS}(\varepsilon) \right]. \quad (3.15)$$

In summary, we have been able to take the limit $\delta \rightarrow 0$, namely to carry the first step of the regularization. This leaves us with the limit $\varepsilon \rightarrow 0$ and the sum over l , which we next consider.

2. The sum over l

The situation in Eq. (3.15) is in some respect similar to the t -splitting variant [10] (see in particular Eq. (3.5) therein). The main difference is that the ω -integral of [10] is here replaced by sum over l . This directly reflects on the way we treat the counter-term: The Fourier decomposition of $G_{DS}(\varepsilon)$ in Ref. [10] will be replaced here by a Legendre decomposition. From Eq. (3.10), we see that the quantities that need be Legendre-expanded are $\sin^{-2}(\varepsilon/2)$ and $\ln[\sin(\varepsilon/2)]$. This decomposition yields (see Appendix C)

$$\sin^{-2}(\varepsilon/2) = -8\pi \sum_{l=0}^{\infty} \frac{2l+1}{4\pi} h(l) P_l(\cos \varepsilon) \quad (3.16)$$

and

$$\ln[\sin(\varepsilon/2)] = 2\pi \sum_{l=0}^{\infty} \frac{2l+1}{4\pi} \Lambda(l) P_l(\cos \varepsilon), \quad (3.17)$$

where $h(l)$ is the *Harmonic Number* given by

$$h(l) \equiv \sum_{k=1}^l \frac{1}{k},$$

(with $h(0) \equiv 0$), and $\Lambda(l)$ is defined to be

$$\Lambda(l) \equiv \begin{cases} -1 & l = 0 \\ -\frac{1}{l(l+1)} & l > 0 \end{cases}.$$

¹⁰ To be more precise, the condition for this vanishing of the l -sum is $\varepsilon \neq n\pi$ for any integer n .

Inserting these identities in Eqs. (3.10) and (3.15) results in

$$\langle \phi^2(x) \rangle_{ren} = \hbar \lim_{\varepsilon \rightarrow 0} \sum_{l=0}^{\infty} \frac{2l+1}{4\pi} P_l(\cos \varepsilon) F_{reg}(l, z) + W(z), \quad (3.18)$$

where

$$W(z) = -\hbar [(\ln(\mu r) + \gamma) c(z) + d(z)], \quad (3.19)$$

$$F_{reg}(l, z) \equiv F(l, z) - F_{sing}(l, z), \quad (3.20)$$

and

$$F_{sing}(l, z) = -8\pi a(z) h(l) + 2\pi c(z) \Lambda(l). \quad (3.21)$$

Note that F_{sing} diverges logarithmically with l , like $h(l)$.

3. “Blind spots” and their self-cancellation

After we have subtracted the singular piece $F_{sing}(l, z)$, one might hope that the sum over l in Eq. (3.18) would now converge even when $\varepsilon = 0$ is substituted in the Legendre polynomial. Unfortunately this is not the case, and one generally finds this sum diverges if $P_l \rightarrow 1$ is substituted. This is demonstrated below in the Schwarzschild case (see e.g. Fig. 2b in Sec. IV). This divergence indicates that the counter-term G_{DS} does not provide full information about the mode-sum singularity (stated in other words, we lose some of the information in the Legendre decomposition). To understand this phenomenon, consider the sum $\sum_{l=0}^{\infty} (2l+1)$ which is obviously divergent, while for any (small) $\varepsilon > 0$

$$\sum_{l=0}^{\infty} (2l+1) P_l(\cos \varepsilon) = 0$$

(see Appendix B; and recall however footnote 10). We shall refer to this phenomenon as a *blind spot*. We define a “blind spot” as a function $B(l)$ for which for any (small) $\varepsilon \neq 0$,

$$\sum_{l=0}^{\infty} (2l+1) B(l) P_l(\cos \varepsilon) = 0,$$

and yet $\sum_{l=0}^{\infty} (2l+1) B(l)$ diverges. In Appendix B we show that all the functions of the form

$$B(l) = \text{const} \cdot [l(l+1)]^n; \quad n = 0, 1, 2, 3, \dots, \quad (3.22)$$

are blind spots. We shall assume that these are the only blind spots that show up in θ -splitting. We cannot prove this assumption, but nevertheless this is the only type we encountered so far in angular splitting (e.g. in Schwarzschild and Reissner-Nordstrom backgrounds, including also in the calculation of $\langle T_{\alpha\beta} \rangle_{ren}$ in these spacetimes). Furthermore, even if one encounters a blind spot of a different type in some background metric, it is reasonable to assume that it will be possible to handle this new type as well.

It is also reasonable to assume that the $\sin^{-2}(\varepsilon/2)$ term in the counter-term should account for the most divergent part in $F(l, r)$. Then we can conclude that the only possible blind spot in the regularization of ϕ^2 corresponds to $n = 0$, namely, $B(l) = \text{const} \equiv B_0(z)$.

We shall assume that this is indeed the case (but note that if blind spots that correspond to other n values happen to show up we know how to self-cancel them as well). We can therefore write

$$F_{reg}(l, z) = B_0(z) + A(l, z), \quad (3.23)$$

where $\sum_{l=0}^{\infty} (2l+1) A(l, z)$ is assumed to be convergent (numerically we find that $A(l, z)$ decays faster than l^{-3}). We can therefore replace $F_{reg}(l, z)$ by $A(l, z)$ in Eq. (3.18). The sum over l in the R.H.S of the latter now converges — even for $\varepsilon = 0$. Presumably we can now interchange the limit with the sum in Eq. (3.18), which then reduces to

$$\langle \phi^2(x) \rangle_{ren} = \hbar \sum_{l=0}^{\infty} \frac{2l+1}{4\pi} A(l, z) + W(z). \quad (3.24)$$

We still need to address one pragmatic issue: The quantity we obtain from the numerics (via Eq. (3.20)) is $F_{reg}(l, z)$ rather than $A(l, z)$. We somehow need to subtract the appropriate quantity $B_0(z)$ from $F_{reg}(l, z)$. In principle we can do this by picking some sufficiently large l value which we denote l_{large} [such that $A(l, z)$ is sufficiently small and can be neglected], and hence approximate $B_0(z)$ by $F_{reg}(l_{large}, z)$; This way, we approximate $A(l, z)$ by $F_{reg}(l, z) - F_{reg}(l_{large}, z)$. We call this strategy “self-cancellation” of the undesired quantity $B_0(z)$.¹¹

We find it more convenient, however, to achieve the self cancellation of B_0 in a slightly different way: We define the sequence of partial sums:

$$H(l, z) \equiv \sum_{k=0}^l \frac{2k+1}{4\pi} [F_{reg}(k, z) - F_{reg}(l, z)]. \quad (3.25)$$

The desired sum over l in Eq. (3.24) is nothing but the limit $l \rightarrow \infty$ of $H(l, z)$:

$$\begin{aligned} \lim_{l \rightarrow \infty} H(l, z) &= \lim_{l \rightarrow \infty} \sum_{k=0}^l \frac{2k+1}{4\pi} [A(k, z) - A(l, z)] \\ &= \sum_{k=0}^{\infty} \frac{2k+1}{4\pi} A(k, z) + \frac{1}{4\pi} \lim_{l \rightarrow \infty} [(l+1)^2 A(l, z)]. \end{aligned}$$

In the last term the limit $l \rightarrow \infty$ vanishes, implying that

$$\lim_{l \rightarrow \infty} H(l, z) = \sum_{l=0}^{\infty} \frac{2l+1}{4\pi} A(l, z).$$

We therefore rewrite Eq. (3.24) in the form

$$\langle \phi^2(x) \rangle_{ren} = \hbar \lim_{l \rightarrow \infty} H(l, z) + W(z). \quad (3.26)$$

We have thus demonstrated how a self-cancellation process can turn the generalized sum with separated points in Eq. (3.18) into a convergent conventional sum/limit at the

¹¹ This is somewhat analogous to the process of oscillation self-cancellation in the t -splitting [10].

coincide, which can be directly computed numerically. We have tailored our self-cancellation procedure to the blind spot we have encountered so far (namely $n = 0$). The generalization to any (integer) $n \geq 1$ is straightforward; and if another type of blind spot shows up in some background, we assume it would be possible to self-cancel it too. Furthermore, methods other than self-cancellation can be used to get rid of the blind spots. One such example is to calculate $B_0(z)$ from leading-order WKB approximation, and subtract it instead of $F_{reg}(l, z)$ in Eq. (3.25).

Let us summarize the result of our regularization procedure: The final expression for $\langle \phi^2(x) \rangle_{ren}$ is given in Eq. (3.26), with $H(l, z)$ defined in Eq. (3.25), where $F_{reg}(l, z)$ and $W(z)$ are specified in (3.19-3.20). The quantity $F_{reg}(l, z)$ is defined using $F_{sing}(l, z)$ of Eq. (3.21) and $F(l, z)$ which is numerically computed according to Eqs. (3.12, 3.13) from the mode functions $\psi_{\omega l}(z)$.

4. The static eternal BH case

In the case of a static eternal BH z runs from ∞ at spacelike infinity to $-\infty$ at the horizon. In this case there are two sets of basis solutions for the radial equation, instead of one. These two sets, which we denote $\psi_{\omega l}^{in}, \psi_{\omega l}^{up}$, are defined by the boundary conditions

$$\begin{aligned} r \sqrt{4\pi\omega} \bar{\psi}_{\omega l}^{in}(z) \equiv \psi_{\omega l}^{in}(z) &= \begin{cases} \tau_{\omega l}^{in} e^{-i\omega z}, & z \rightarrow -\infty \\ e^{-i\omega z} + \rho_{\omega l}^{in} e^{i\omega z}, & z \rightarrow \infty \end{cases} \\ r \sqrt{4\pi\omega} \bar{\psi}_{\omega l}^{up}(z) \equiv \psi_{\omega l}^{up}(z) &= \begin{cases} e^{i\omega z} + \rho_{\omega l}^{up} e^{-i\omega z}, & z \rightarrow -\infty \\ \tau_{\omega l}^{up} e^{i\omega z}, & z \rightarrow \infty \end{cases} \end{aligned} \quad (3.27)$$

where $\tau_{\omega l}, \rho_{\omega l}$, represent the transmission and reflection amplitudes.

The *Boulware state* is the vacuum state that is naturally associated to the $\psi_{\omega l}^{in}, \psi_{\omega l}^{up}$ modes. Thus, applying the angular splitting in this state is almost identical to the prescription given above. The only thing that requires modification is Eq. (3.12), which should now contain the two sets of modes:

$$E_{\omega l}(z) \equiv |\bar{\psi}_{\omega l}^{in}(z)|^2 + |\bar{\psi}_{\omega l}^{up}(z)|^2. \quad (3.28)$$

We point out that in the eternal case too the leading order large- ω contribution of the modes is independent of l . As can be seen in Appendix D (see end of Sec. D 1), both $|\bar{\psi}_{\omega l}^{in}|^2$ and $|\bar{\psi}_{\omega l}^{up}|^2$ are dominated by $1/(4\pi r^2 \omega)$; In fact their sum

$$E_{\omega l} \cong \frac{1}{2\pi r^2 \omega} \quad (3.29)$$

is the same as in the regular-center case, Eq. (3.7). Hence the method of regularizing the ω -integral by $l = 0$ subtraction works equally well in the eternal case. Thus we again define $F(l, z)$ according to Eq. (3.13), and then proceed with the calculation of $\langle \phi^2 \rangle_{ren}$ just as described in the previous subsection.

To calculate $\langle \phi^2 \rangle_{ren}$ in the Unruh or Hartle-Hawking state, in the right-hand side of Eq. (3.28) one simply multiplies $|\bar{\psi}_{\omega l}^{up}|^2$, and in Hartle-Hawking state also $|\bar{\psi}_{\omega l}^{in}|^2$, by the factor $\coth(\pi\omega/\kappa)$, where κ is the BH's surface gravity, as described in Eqs. (4.4, 4.5) below.

B. The time-dependent spherically symmetric case

Generalizing the method presented in Sec. III A we now consider the generic, dynamical, asymptotically-flat spherically-symmetric metric (2.2), along with the field decomposition given in Eq. (2.9). We start with the case of a spacetime with a regular center, treating the eternal-BH case later on. The static mode functions $\bar{\psi}_{\omega l}(z)$ are now replaced by $\bar{\Psi}_{\omega l}(t, z)e^{i\omega t}$. Therefore the time-dependent analog of the point-splitting expression for $\langle \phi^2(x) \rangle_{ren}$ (summed over m), Eq. (3.8), is

$$\langle \phi^2 \rangle_{ren} = \lim_{\varepsilon \rightarrow 0} \left[\lim_{\delta \rightarrow 0} \hbar \sum_{l=0}^{\infty} \frac{2l+1}{4\pi} P_l(\cos \varepsilon) \int_0^\infty \bar{\Psi}_{\omega l}(t, z) \bar{\Psi}_{\omega l}^*(t + \delta, z) d\omega - G_{DS}(\varepsilon) \right]. \quad (3.30)$$

The biscalar $\sigma(\varepsilon)$ and the counter-term $G_{DS}(\varepsilon)$ take the same form as in Eqs. (3.9)-(3.10), except that the parameters are now functions of both t and z . In particular \tilde{c} and c, d are now given by

$$\begin{aligned} \tilde{c}(t, z) &= \frac{r^2}{24\Gamma} (\dot{r}^2 - r'^2) , \\ c(t, z) &= \frac{(1/6 - \xi)}{8\pi^2 r^2 \Gamma^3} \left\{ -2\Gamma^3 + r^2 (\dot{\Gamma}^2 - \Gamma'^2) + r^2 \Gamma (-\ddot{\Gamma} + \Gamma'') \right. \\ &\quad \left. + 2\Gamma^2 (-\dot{r}^2 + r'^2) + 4r\Gamma^2 (-\ddot{r} + r'') \right\} , \\ d(t, z) &= \frac{1}{48\pi^2 r \Gamma} (\ddot{r} - r'') . \end{aligned}$$

(The parameter a is unchanged.)

The large- ω asymptotic behavior of $|\bar{\Psi}_{\omega l}|$ is addressed in Appendix D. In the case of a background with regular center (either static or time dependent), the leading-order term is given in Eq. (D6). Its integral over ω diverges logarithmically, but again it is independent of l . Hence, here too we subtract and add the $l = 0$ mode, after which the integral over ω in Eq. (3.30) takes the form

$$\begin{aligned} \int_0^\infty [\bar{\Psi}_{\omega l}(t, z) \bar{\Psi}_{\omega l}^*(t + \delta, z) - \bar{\Psi}_{\omega, l=0}(t, z) \bar{\Psi}_{\omega, l=0}^*(t + \delta, z)] d\omega \\ + \int_0^\infty \bar{\Psi}_{\omega, l=0}(t, z) \bar{\Psi}_{\omega, l=0}^*(t + \delta, z) d\omega. \end{aligned}$$

The second integral is independent of l , hence as explained above it yields zero contribution upon summation over l (for finite ε). The first integral converges even for $\delta = 0$, so we simply insert the limit $\delta \rightarrow 0$ in the integrand. Thus, the integral over ω in the above expression for $\langle \phi^2 \rangle_{ren}$ reduces to

$$F(l, t, z) \equiv \int_0^\infty d\omega [E_{\omega l}(t, z) - E_{\omega, l=0}(t, z)],$$

where $E_{\omega l}(t, z)$ is defined as the integrand at the coincide:

$$E_{\omega l}(t, z) \equiv |\bar{\Psi}_{\omega l}(t, z)|^2, \quad (3.31)$$

similar to Eq. (3.12). Equation (3.30) now takes the form

$$\langle \phi^2(x) \rangle_{ren} = \lim_{\varepsilon \rightarrow 0} \left[\hbar \sum_{l=0}^{\infty} \frac{2l+1}{4\pi} P_l(\cos \varepsilon) F(l, t, z) - G_{DS}(\varepsilon) \right],$$

similar to Eq. (3.15) in the static case.

From here on the method exactly follows the line described in Sec. III A, except that all the z -dependent quantities will now depend on t as well. Summarizing the main expressions

$$\langle \phi^2(x) \rangle_{ren} = \hbar \lim_{l \rightarrow \infty} H(l, t, z) + W(t, z),$$

where

$$H(l, t, z) \equiv \sum_{k=0}^l \frac{2k+1}{4\pi} [F_{reg}(k, t, z) - F_{reg}(l, t, z)],$$

$$W(t, z) \equiv -\hbar [(\ln(2\mu r) + \gamma) c(t, z) + d(t, z)],$$

and

$$F_{reg}(l, t, z) \equiv F(l, t, z) - F_{sing}(l, t, z),$$

$$F_{sing}(l, t, z) = -8\pi a(t, z) h(l) + 2\pi c(t, z) \Lambda(l).$$

The dynamical eternal-BH case

Similar to the static case, in a dynamical eternal-BH background there are two sets of basis solutions $\bar{\Psi}_{\omega l}^{in}(t, z), \bar{\Psi}_{\omega l}^{up}(t, z)$. The initial conditions for these solutions are easy to express in double-null coordinates:

$$\lim_{pni} \Psi_{\omega l}^{in}(u, v) = e^{-i\omega v}, \quad \lim_{ph} \Psi_{\omega l}^{in}(u, v) = 0 \quad (3.32)$$

and

$$\lim_{ph} \Psi_{\omega l}^{up}(u, v) = e^{-i\omega u}, \quad \lim_{pni} \Psi_{\omega l}^{up}(u, v) = 0, \quad (3.33)$$

where “pni” and “ph” stand for “past null infinity” and “past horizon” respectively.¹² Thus the only change required from the non-eternal dynamical case described above is in Eq. (3.31), which is now replaced by

$$E_{\omega l}(t, z) \equiv |\bar{\Psi}_{\omega l}^{in}(t, z)|^2 + |\bar{\Psi}_{\omega l}^{up}(t, z)|^2.$$

Note that in a static background the Eddington-like null coordinates u, v are naturally defined by the time translation symmetry, but in a dynamical eternal-BH background this definition no longer holds. The coordinate v is still naturally defined by asymptotic flatness at PNI (and indeed we assume this definition of v throughout), but u is no longer uniquely defined. The boundary conditions in Eq. (3.33) thus induce a vacuum state that depends on the specific choice of the u coordinate, via the definition of the $\Psi_{\omega l}^{up}$ modes. This ambiguity in the choice of vacuum does not arise in the non-eternal case (and certainly not in the static case).¹³

¹² The vacuum state naturally associated to this set of modes is the (time-dependent analog of the) Boulware state.

¹³ One may choose to define u via asymptotic flatness at FNI, but it is not clear if this will always be

IV. APPLICATION TO THE SCHWARZSCHILD CASE

We now demonstrate the implementation of the angular-splitting variant by calculating $\langle \phi^2(x) \rangle_{ren}$ in the exterior of a Schwarzschild spacetime, for a massless scalar field.¹⁴ We do this first in the Boulware vacuum, and later on in Sec. IV B we also give results for the Unruh and Hartle-Hawking states. The Schwarzschild metric is

$$ds^2 = - \left(1 - \frac{2M}{r}\right) dt^2 + \left(1 - \frac{2M}{r}\right)^{-1} dr^2 + r^2 d\Omega^2,$$

where M is the BH mass. Defining the usual tortoise coordinate

$$r_* = r + 2M \ln \left(\frac{r}{2M} - 1 \right)$$

the metric can be written as

$$ds^2 = \left(1 - \frac{2M}{r}\right) (-dt^2 + dr_*^2) + r^2 d\Omega^2.$$

Thus, in the Schwarzschild case the coordinates z used below can be replaced by the more familiar symbol r_* . Also, since in the exterior of Schwarzschild $r(r_*)$ is a monotonically increasing function, it is now possible (and it is often convenient) to use r as a radial variable. (Which is not the case in the general static case, where $r(z)$ need not be monotonic.)

The radial equation for the modes is as given in Eq. (3.3),

$$\psi''_{\omega l}(r) = [V_l(r) - \omega^2] \psi_{\omega l}(r), \quad (4.1)$$

where a prime denotes $d/dz \equiv d/dr_*$, and the effective potential in the Schwarzschild case takes the form

$$V_l(r) = \left(1 - \frac{2M}{r}\right) \left[\frac{l(l+1)}{r^2} + \frac{2M}{r^3} \right].$$

The Schwarzschild geometry describes an eternal BH, so there are two sets of basis solutions $\bar{\psi}_{\omega l}^{in}, \bar{\psi}_{\omega l}^{up}$ and the scheme is executed following Sec. III A 4. For the Schwarzschild background (and for $m = 0$) the parameters $a(r), c(r), d(r)$ take the simple forms

$$a(r) = \frac{1}{16\pi^2 r^2}, \quad c(r) = 0, \quad d(r) = -\frac{M}{24\pi^2 r^3}.$$

For reference we also give here the explicit expressions for $F_{sing}(l, r)$ and $W(r)$:

$$F_{sing}(l, r) = -\frac{1}{2\pi r^2} h(l), \quad W(r) = \hbar \frac{M}{24\pi^2 r^3}. \quad (4.2)$$

Then $\langle \phi^2 \rangle_{ren}$ is given by Eq. (3.26).

the most convenient choice. Another natural candidate is the log of the affine parameter along the past horizon. In the non-eternal case a natural choice of u may arise from the requirement that the center of symmetry would be placed at $z = 0$.

¹⁴ Note that in Schwarzschild $\langle \phi^2 \rangle_{ren}$ does not depend on ξ because $R = 0$.

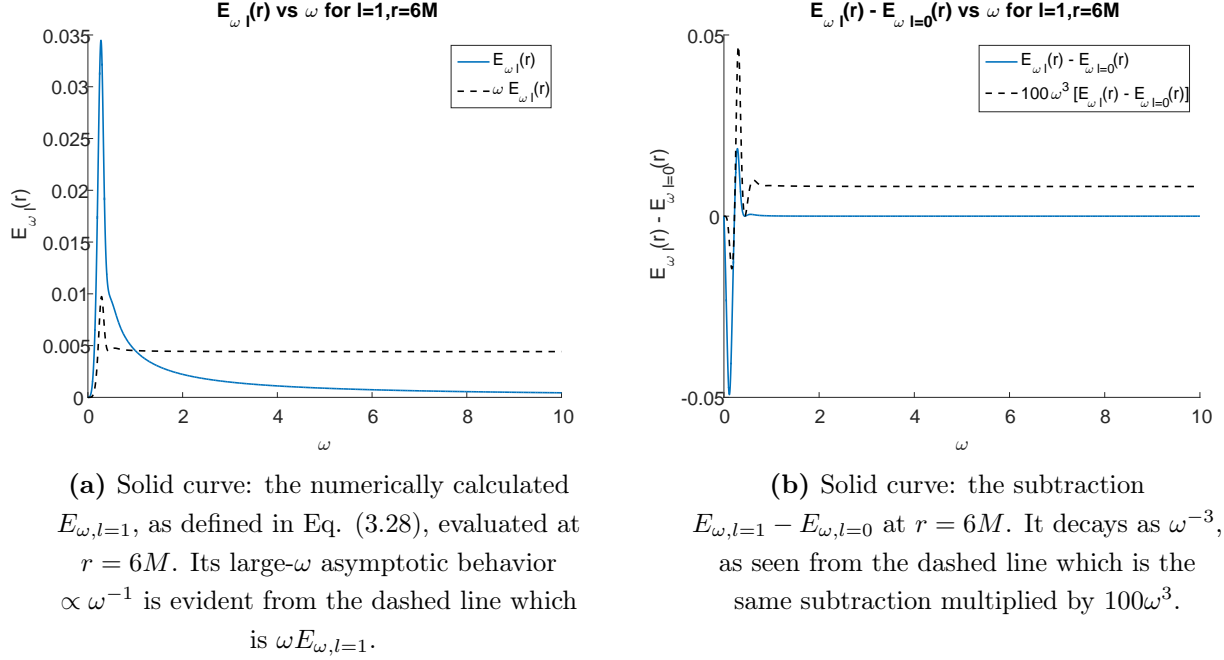


Figure 1:

A. Numerical implementation in Schwarzschild

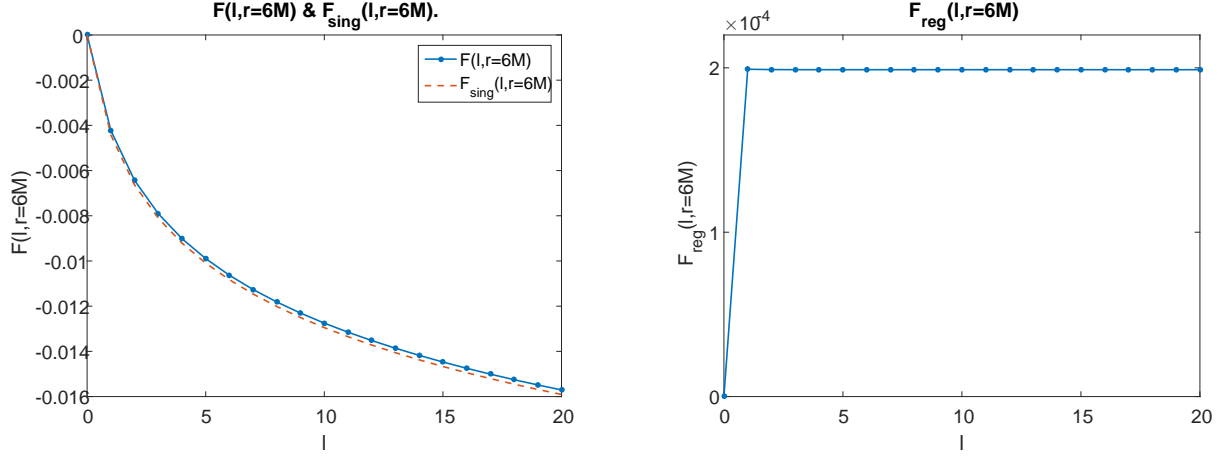
The radial equation (4.1) was numerically solved for $\psi_{\omega l}(r)$ using MATHEMATICA's ODE solver. It was solved for 21 different l values ($0 \leq l \leq 20$), and for each l in the range $\omega \in [0, 10]$, with a uniform spacing $d\omega = 1/1000$,¹⁵ namely $\sim 2 \cdot 10^5$ modes. In all graphs below we use units where $M = 1$, in addition to $G = c = 1$.

As an example we follow the calculation for $r = 6M$ in Boulware state, illustrating the various stages of the regularization process. Figure 1a displays $E_{\omega l}$ for $l = 1$. This quantity behaves like $1/\omega$ at large ω (see dashed curve), so its integral would diverge at infinity. It is regularized according to Eq. (3.13) by subtracting from it the $l = 0$ mode; the resultant integrand behaves as $1/\omega^3$ for large ω , as seen in Fig. 1b (dashed curve).

Although the ω -integral of $E_{\omega l}(r) - E_{\omega,l=0}(r)$ is convergent, it does not converge sufficiently fast, due to the ω^{-3} tail. This would bring up the need for a much longer range in ω (and hence a much larger number of modes) in order to achieve a sufficient accuracy of the integral. To overcome this difficulty, we carried the large- ω expansion of $\psi_{\omega l}(r)$ up to order ω^{-8} , and used this analytical approximation for evaluating the integral from $\omega = 10$ to infinity. This expansion is described in Appendix D, see in particular Eqs. (D2-D4). This is one way to obtain a more accurate result with a limited range in ω , but one can also think of other ways.

The result of the integration over ω is $F(l, r)$, seen in Fig. 2a. As expected it behaves

¹⁵ Note that in most cases one does not need to go up to $l = 20$, usually the convergence is much faster. We found, however, that for large r values in the Hartle-Hawking state the convergence in l is slower so that we needed the modes up to $l = 20$ to keep the high accuracy. We also note that a spacing of $d\omega = 1/1000$ is really unnecessary and one can get excellent accuracy even with $d\omega = 1/100$.



(a) The solid curve represents $F(l, r = 6M)$, calculated according to Eq. (3.13). The dashed curve is the analytic function $F_{\text{sing}}(l, r = 6M)$, given in Eq. (4.2).

(b) The graph displays $F_{\text{reg}}(l, r = 6M)$, which is simply the difference between the two curves in Fig. 2a. It rapidly approaches a constant, the “blind-spot” discussed in Sec. III A 3.

Figure 2:

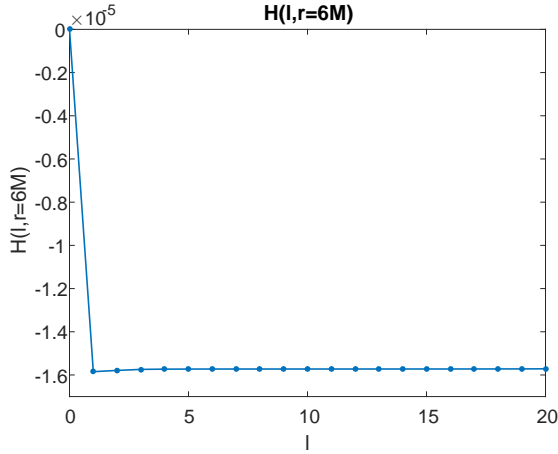
logarithmically for large l (like $F_{\text{sing}}(l, r)$), and the sum over l of $(2l + 1) F(l, r)$ is of course divergent. The subtraction of $F_{\text{sing}}(l, r)$ according to Eq. (3.20) eliminates most of the divergent part of $F(l, r)$. The result is $F_{\text{reg}}(l, r)$, which asymptotically behaves like a constant (Fig. 2b). This fits our understanding of the blind-spot and matches the structure of Eq. (3.23).

Next we self-cancel the blind spot by constructing $H(l, r)$ according to Eq. (3.25). It is clear from Fig. 3a that the sequence $H(l, r)$ indeed converges as anticipated; furthermore, it converges very fast as can be seen from the zoom in Fig. 3b. After the large- l limit of $H(l, r)$ is computed, $\langle \phi^2 \rangle_{\text{ren}}$ is calculated according to Eq. (3.26).

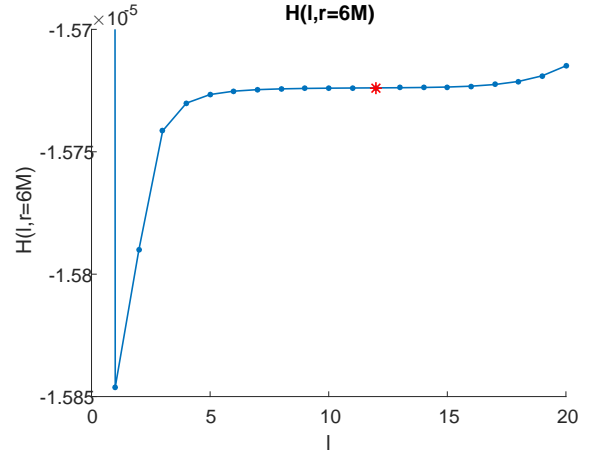
In Fig. 4a we present $\langle \phi^2 \rangle_{\text{ren}}$ as a function of r in Boulware state, for various r values between $2.03M$ and $40M$ ¹⁶, and compare it to previous results calculated using the t -splitting variant [10]. The two variants admit excellent agreement and the difference is typically of order one part in 10^4 .¹⁷ We also compare our results to the ones calculated by Anderson [15] using an entirely different method (WKB expansion in the euclidean sector), which also admits very good agreement. The near-horizon asymptotic behavior of $\langle \phi^2 \rangle_{\text{ren}}$ in Boulware state is shown in Fig. 4b; as expected it diverges like $(1 - 2M/r)^{-1}$ so we

¹⁶ Our numerical results get close to the horizon up to $r = 2.001M$. However, in the Boulware state we give the results only up to $2.03M$ because closer than that the accuracy deteriorates rapidly. This is expected due to the divergence of the Boulware state on approaching the horizon.

¹⁷ This does not necessarily mean that the error in the numerically evaluated $\langle \phi^2 \rangle_{\text{ren}}$ is that small. The error may turn out to be larger than the difference between the two variants. For example, a numerical error in evaluating the contribution from any mode that we include in both splittings, will yield same error in the two variants and will not show up in their difference. Nevertheless, from various indicators we estimate that the error is typically around one part in 10^3 or smaller.



(a) The sequence $H(l, r)$ constructed according to Eq. (3.25). The fast convergence is evident.



(b) A close-up on the plateau in Fig. 3a. In this zoom one can also notice the growth of numerical error at large l (say $l > 16$). The red cross indicates the estimated optimal l value (for numerically evaluating the large- l limit of $H(l, r)$; $l = 12$ in the present case).

This estimated optimal l is automatically selected by an algorithm that assesses where the numerical error starts to grow.

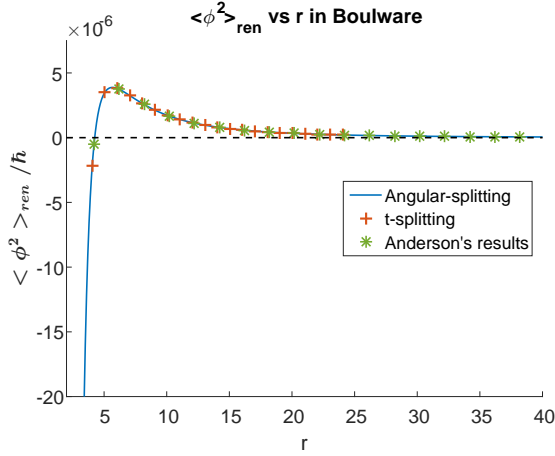
Figure 3:

plot $(1 - 2M/r) \langle \phi^2 \rangle_{ren}$ which is finite. There is good visual agreement with the known limiting value $-\hbar/(768\pi^2 M^2)$ (the dotted horizontal line in Fig. 4b) at $r = 2M$, calculated analytically by Candelas [12].

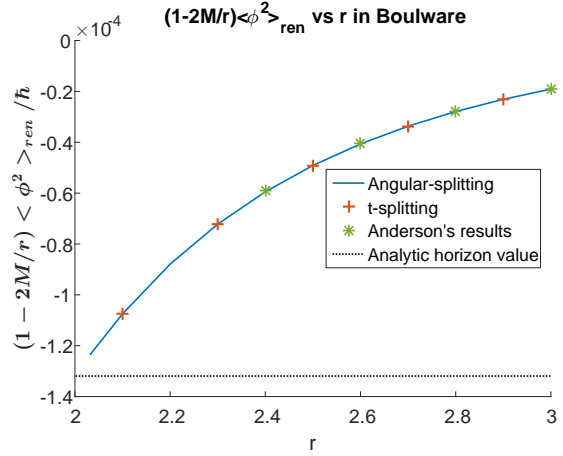
B. Unruh and Hartle-Hawking states

In addition to the Boulware state, we also used the angular splitting method to calculate $\langle \phi^2 \rangle_{ren}$ in the Unruh and Hartle-Hawking vacuum states. The regularization process is the same as the one described above for the Boulware state; the only difference is in the mode contributions. In principle each vacuum state is established on different sets of basis modes, defined according to different boundary conditions. Nevertheless it is not necessary to re-solve the differential equations for the mode functions for each state separately: One can construct the mode contributions for the Hartle-Hawking and Unruh states from the same set of solutions $\psi_{\omega l}^{in}(r)$, $\psi_{\omega l}^{up}(r)$ that we used for the Boulware state. We give here the mode contributions in the different vacuum states and refer the reader to derivation of these relations by Christensen and Fulling [11]:

$$E_{\omega l}^{Boulware}(r) \equiv |\bar{\psi}_{\omega l}^{in}(r)|^2 + |\bar{\psi}_{\omega l}^{up}(r)|^2, \quad (4.3)$$



(a) The solid line represents the results for $\langle \phi^2 \rangle_{ren}$ in the Boulware state, calculated using the new angular-splitting variant. There is excellent agreement with both the results obtained using the t -splitting variant (the crosses) and previous results by Anderson (the asterisks).



(b) A near horizon close-up of $(1 - 2M/r) \langle \phi^2 \rangle_{ren}$, showing that it is clearly finite. Here we also give the analytic horizon value calculated by Candelas (the dotted line).

Figure 4:

[which is actually the original function $E_{\omega l}$ given in Eq. (3.28)], and

$$E_{\omega l}^{Unruh}(r) \equiv |\bar{\psi}_{\omega l}^{in}(r)|^2 + \coth\left(\frac{\pi\omega}{\kappa}\right) |\bar{\psi}_{\omega l}^{up}(r)|^2, \quad (4.4)$$

$$E_{\omega l}^{H-H}(r) \equiv \coth\left(\frac{\pi\omega}{\kappa}\right) \left(|\bar{\psi}_{\omega l}^{in}(r)|^2 + |\bar{\psi}_{\omega l}^{up}(r)|^2 \right), \quad (4.5)$$

where κ is the surface gravity of the black hole, in Schwarzschild $\kappa = 1/(4M)$. Notice that the regularization in ω does not require any modification since the large- ω asymptotic behavior is the same for the three vacuum states, as $\coth(\pi\omega/\kappa)$ exponentially approaches one at large ω .

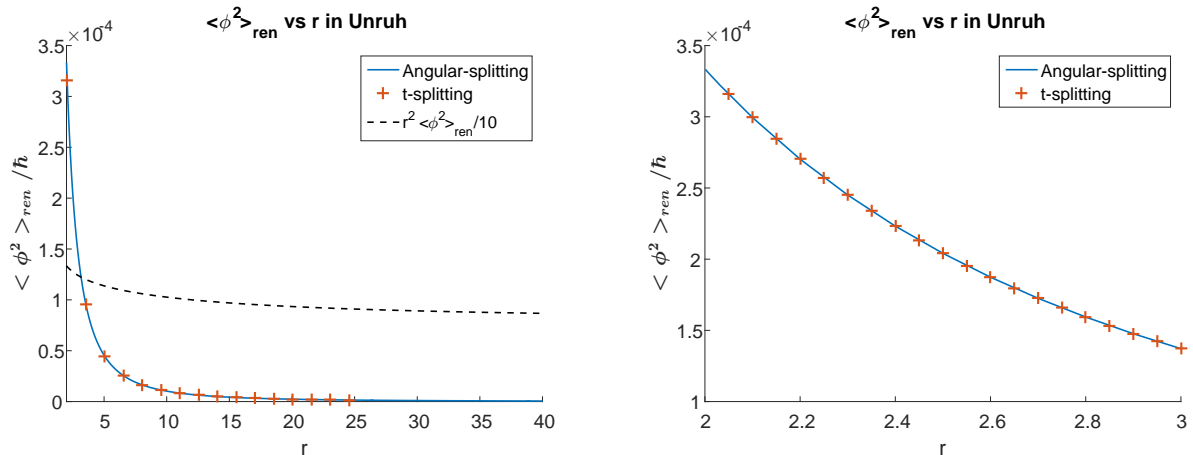
Figure 5a displays $\langle \phi^2(r) \rangle_{ren}$ in the Unruh state, along with results calculated using the t -splitting variant. The agreement is again excellent and the difference is typically a few parts in 10^5 . From this figure one might get the wrong visual impression that $\langle \phi^2 \rangle_{ren}$ diverges at $r \rightarrow 2M$. To show that this is not the case, Fig. 5b zooms on the closer neighborhood of the horizon and demonstrates the regularity of $\langle \phi^2(r) \rangle_{ren}$ as $r \rightarrow 2M$.

For future reference we also give here the horizon value extrapolated from the points calculated near the horizon:

$$\langle \phi^2(r = 2M) \rangle_{ren}^{Unruh} \approx 3.336 \cdot 10^{-4} \frac{\hbar}{M^2}.$$

In addition, the leading-order asymptotic behavior at infinity was extrapolated and found to be

$$\langle \phi^2(r \rightarrow \infty) \rangle_{ren}^{Unruh} \approx 7.763 \cdot 10^{-4} \frac{\hbar}{r^2}.$$



(a) The solid curve displays $\langle \phi^2 \rangle_{ren}$ in Unruh state calculated using angular splitting. The results obtained using the t -splitting variant are marked by crosses. The dashed curve is aimed to demonstrate the $\propto (r^{-2})$ large- r asymptotic behavior of $\langle \phi^2 \rangle_{ren}$, by multiplying the latter by $r^2/10$.

(b) A near-horizon zoom on $\langle \phi^2 \rangle_{ren}$ in Unruh state, demonstrating its regularity at $r \rightarrow 2M$.

Figure 5:

Candelas gave analytic expressions for the asymptotic behavior at the horizon and at infinity. These two asymptotic expressions depend on the gray-body factor (see Table I in Ref [12]). Nevertheless we find that there exists a combination, which we denote by χ , that cancels the gray-body factor and yields an explicit analytic value. This combination is

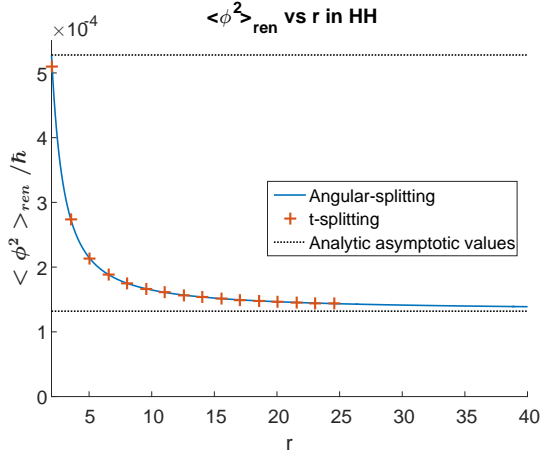
$$\chi = \langle \phi^2(r = 2M) \rangle_{ren}^{Unruh} + \frac{r^2}{4M^2} \langle \phi^2(r \rightarrow \infty) \rangle_{ren}^{Unruh} = \frac{\hbar}{192\pi^2 M^2}.$$

The numerically calculated results agree with this analytic value to about one part in 10^4 .

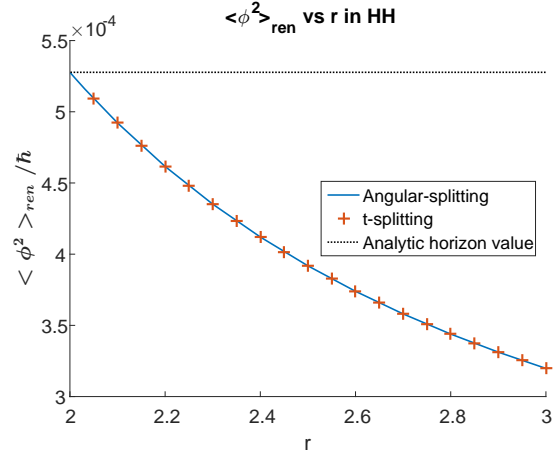
Finally we also display $\langle \phi^2 \rangle_{ren}$ in the Hartle-Hawking state in Fig. 6a. Again the deviations from the calculation using the t -splitting variant are typically a few parts in 10^5 . The figure also shows the asymptotic values analytically calculated by Candelas [12] at infinity ($\hbar/768\pi^2 M^2$) and at the horizon ($\hbar/192\pi^2 M^2$). Similar to the Unruh state the value at the horizon is finite, this is clearly visible in Fig. 6b. We have calculated the limiting values at $r = 2M$ and at $r \rightarrow \infty$, and these extrapolated numerical values agree with Candelas' analytical results up to two parts in 10^5 and three part in 10^4 respectively.

V. DISCUSSION

This paper is the second in a series that presents a new approach for numerically implementing the point-splitting regularization scheme in asymptotically flat spacetimes of black holes, or other compact objects. Our approach only requires the background to admit some symmetry, one which allows (even partial) separation of variables in the field equation.



(a) The solid curve displays $\langle \phi^2 \rangle_{ren}$ in the Hartle-Hawking state calculated using the angular-splitting method. The results obtained from the t -splitting variant are marked by crosses. The analytical asymptotic values calculated by Candelas are represented by the two dotted horizontal lines (top line — horizon; bottom line — infinity).



(b) A near-horizon zoom on $\langle \phi^2 \rangle_{ren}$ in the Hartle-Hawking state. One can see the agreement with the analytical value at the horizon calculated by Candelas (the dotted horizontal line).

Figure 6:

The first paper [10] presented the regularization of $\langle \phi^2 \rangle$ in the t -splitting variant designed for stationary backgrounds; here we presented the regularization of this same quantity in the θ -splitting variant, applicable to spherically symmetric backgrounds. In both cases we restricted our attention to $\langle \phi^2 \rangle$ for simplicity. In forthcoming papers we shall apply our method to the renormalized stress-energy tensor. We also hope to present a third variant, azimuthal splitting, which would be usable for generic axially-symmetric backgrounds.

To demonstrate how the θ -splitting method works in practice, we applied it here to the Schwarzschild case, and calculated $\langle \phi^2 \rangle_{ren}$ in all three vacuum states: Boulware, Hartle-Hawking, and Unruh. The results were found to agree very well with our previous results obtained from t -splitting, and also with results calculated by Anderson using a very different method [15] — as well as with known analytical results [12] at the horizon and at infinity.

At the technical level, there is a notable difference between the t -splitting and θ -splitting variants: In the former, as long as the points are separated (in t), the mode-sum operations are regular. In θ -splitting, by contrast, the integral over ω diverges despite the separation in θ . To handle this intermediate-stage divergence we had to introduce an additional, auxiliary, separation in t (which we take to vanish before taking the θ -separation to zero). This makes the θ -splitting variant slightly more complicated than its t -splitting counterpart — nevertheless not too complicated, as demonstrated by the Schwarzschild example.

The analytical processing of the point-separated expression for $\langle \phi^2 \rangle_{ren}$ in Sec. III A involved a key manipulation: We have interchanged the order of the $\delta \rightarrow 0$ limit in Eq. (3.8) with the sum over l , and also with the integral over ω . [This interchange led to elimination of the factor $e^{i\omega\delta}$ in the first integral in the R.H.S. of Eq. (3.11), replacing this integral by

$F(l)$, hence leading to Eq. (3.15).] We are unable to provide a rigorous mathematical proof for the justification of this interchange. The main obstacle, of course, is the fact that the functions $\bar{\psi}_{\omega l}(z)$ are not known explicitly. Nevertheless, we do find strong evidence for the validity of this interchange. It is fairly clear that the justification (or otherwise) of such an interchange would primarily depend on the asymptotic behavior of the function $|\bar{\psi}_{\omega l}(z)|^2$ at large l and large ω . (For instance, if this function were vanishing beyond some l , the sum would then become a finite one and its interchange with the $\delta \rightarrow 0$ limit would be a trivial operation.) This domain of large l and large ω is amenable to WKB analysis. It therefore seems reasonable to assume that for the sake of addressing this interchangeability issue, one could represent $\bar{\psi}_{\omega l}(z)$ by its leading-order WKB approximation. Preliminary investigation of this issue within leading-order WKB suggests to us that the $\delta \rightarrow 0$ limit is indeed interchangeable with the other operations, justifying our manipulation in Sec. III A. We hope to present the details of this WKB-based analysis elsewhere. An independent strong evidence for the validity of this operation comes from the excellent agreement between the results obtained from θ -splitting and t splitting (and between both of them and previous results by Anderson [15]). This was demonstrated in Sec. IV A for the Schwarzschild case, and similar agreement was also found in the Reissner-Nordstrom case.

We consider the angular-splitting method to be a primary tool in the investigation of self-consistent semiclassical BH evaporation: Since an evaporating BH constitutes a time-dependent background, the t -splitting variant is inapplicable to it (at least in the strict direct sense). Yet the angular-splitting variant should be applicable to this system, owing to its spherical symmetry.

Acknowledgment

We would like to thank Paul Anderson for sharing his unpublished numerical results with us, and also for his kind hospitality and fruitful discussions during our visit at Wake Forest University. This research was supported by the Asher Fund for Space Research at the Technion.

Appendix A: Generalized sums and integrals

As was already mentioned above, all the infinite sums in this paper are in principle *generalized sums*, defined according to *Abel summation method*. Namely, by denoting $\sum_{l=0}^{l=\infty} f(l)$ we actually mean

$$\lim_{\alpha \rightarrow 0^+} \sum_{l=0}^{l=\infty} e^{-\alpha l} f(l).$$

The same applies to the integrals over ω : By denoting $\int_0^\infty f(\omega) d\omega$ we actually refer to the corresponding *generalized integral* defined as

$$\lim_{\alpha \rightarrow 0^+} \int_0^\infty e^{-\alpha \omega} f(\omega) d\omega.$$

The reason for using such generalized sums and integrals is the presence of undamped oscillations at large l or large ω , as explained in Sec. II C.

Some of the sums/integral in the paper do converge in the conventional sense. Note that no ambiguity arises in such cases from the usage of the same symbol “ \sum ” (“ \int ”) for both the conventional sum (integral) and the generalized one, due to the following consistency property: Whenever a sum/integral converges in the usual sense, it is guaranteed to coincide with the corresponding generalized sum/integral.

The oscillations in the summation of various quantities over l usually arise from the oscillatory nature of the Legendre factor $P_l(\cos\varepsilon)$. Therefore these oscillations disappear when $\varepsilon \rightarrow 0$ is substituted. Since at the end of the day all the numerical calculations of the mode functions are carried in this coincidence limit, it follows that eventually no undamped oscillations in l are encountered in the numerical evaluation part. (These large- l oscillations only appear in the preceding, theoretical part of the analysis that involves the usage of separated θ , namely $\varepsilon \neq 0$.)

The situation with regards to the oscillations at large ω is somewhat different, as we now discuss.

1. Large- ω oscillations

The oscillations in the integrals of various quantities over ω arise from a more geometric reason: The presence of a null geodesic that connects pairs of points separated in t only. The two-point function diverges for such null-separated points, leading to large- ω oscillations in its Fourier decomposition (see [10]). Strong ($\propto \omega^{1/2}$) such large- ω oscillations were encountered, for example, in t splitting. Unlike the oscillations in l , these ω -oscillations survive even at the limit $t' \rightarrow t$. Therefore, whenever these oscillations occur, they show up even in the final stage of numerical integration (which is carried after coincidence). In Ref. [10] we described how we practically implement the generalized integral — and thereby kill the ω -oscillations — by the “self-cancellation” process.

In the present variant of θ splitting the large- ω oscillations are less severe. The main reason is that here we carry the integral over ω for each l separately. The quantities that we integrate are the (square of the absolute value of the) mode functions, namely solutions of a wave equations, in a fictitious 1+1 spacetime (spanned by the t, z coordinates; and with some l -dependent effective potential). By contrast, in t splitting the ω -integration is carried *after* summation over l, m , hence the relevant “effective spacetime” for this manipulation is the true 3+1 spacetime. Owing to the smaller effective dimension in θ splitting, the divergence of the null-connected two-point function is weaker (it is $\propto \ln \sigma$ compared to $1/\sigma$), and so do the large- ω oscillations in its Fourier decomposition.

Indeed, in θ -splitting the oscillations in the integrand $|\bar{\psi}_{\omega l}|^2$ decay as $1/\omega$ in the regular-center case [see Sec. D 2 b, and particularly the Minkowski example (D8)], and are hence integrable;¹⁸ And in the eternal case there are no large- ω oscillations at all. Therefore, self-cancellation of large- ω oscillations is not compulsory in θ -splitting. (However, in the regular-center case, due to the $\propto \omega^{-1}$ oscillations the integral over ω converges rather slowly, and self-cancellation of oscillations is practically needed to speed the convergence.)

Finally we briefly address the reason, from the geometrical view-point, for the presence of large- ω oscillations in the regular-center case, and their absence in the eternal case. As already mentioned above, this may be related to the presence (or otherwise) of null geodesics

¹⁸ By contrast, in t splitting the oscillations diverge as $\omega^{1/2}$. [10]

connecting pairs of points separated by t only, *in the effective 1+1 spacetime* spanned by t and z (which is the relevant effective spacetime for the ω -integration in θ splitting).

We first need to recall that in 1+1 dimensions, genuine connecting null geodesics do not exist at all. This follows immediately from the timelike character of the t -separation, combined with the trivial nature of the light cone in 2d spacetimes. This explains the lack of oscillations in the eternal case.

The situation in backgrounds with a regular center is more delicate, however: Recall that in the effective 1+1 spacetime the high-frequency wave packets (which usually propagate along null geodesics) actually bounce when they hit the origin. Hence, the relevant orbits in the geometrical-optics limit are the “broken” null geodesics, which bounce at the origin. The existence of such “broken connecting null geodesics” (for pairs of points separated in t) leads to large- ω oscillations in the regular-center case.

Nevertheless, note that there is exactly one such “broken connecting null geodesic” — and hence exactly one oscillation frequency — at each point z . This is illustrated, for example, in the Minkowski case (D8). (For comparison, in t splitting in e.g. Schwarzschild background there is an infinite discrete set of connecting null geodesics, and hence infinite set of oscillation frequencies, at each point. [10])

Appendix B: Legendre blind spots

In this Appendix we prove that the generalized sum

$$\sum_{l=0}^{\infty} (2l+1) [l(l+1)]^n P_l(\cos\varepsilon)$$

vanishes for any integer $n \geq 0$.

We first treat the $n = 0$ case, namely we prove that

$$\sum_{l=0}^{\infty} (2l+1) P_l(\cos\varepsilon) = 0. \quad (\text{B1})$$

It is helpful to use the generating function $G(\varepsilon, t)$ (see Ref. [13]) which for any finite ε ($\varepsilon \neq n\pi$) takes the form

$$\sum_{l=0}^{\infty} P_l(\cos\varepsilon) t^l = \frac{1}{\sqrt{1 - 2t\cos\varepsilon + t^2}} \equiv G(\varepsilon, t). \quad (\text{B2})$$

This sum is a *conventional* one (and the same applies to all sums up to Eq. (B3) inclusive); and it converges uniformly throughout the range $0 < t < 1$, which we consider here. Differentiating both sides with respect to t and then multiplying by t we get

$$\sum_{l=0}^{\infty} l P_l(\cos\varepsilon) t^l = t \frac{\partial G(\varepsilon, t)}{\partial t} = \frac{t \cos\varepsilon - t^2}{(1 - 2t\cos\varepsilon + t^2)^{3/2}}.$$

We can now take a combination of the last two equations:

$$\sum_{l=0}^{\infty} (2l+1) P_l(\cos\varepsilon) t^l = 2t \frac{\partial G(\varepsilon, t)}{\partial t} + G(\varepsilon, t) = \frac{1 - t^2}{(1 - 2t\cos\varepsilon + t^2)^{3/2}}.$$

Next we define $\alpha \equiv -\ln t$, noting that $\alpha > 0$ in the relevant domain. Substituting $t = e^{-\alpha}$ in the last equation yields

$$\sum_{l=0}^{\infty} (2l+1) P_l(\cos \varepsilon) e^{-\alpha l} = \frac{1 - e^{-2\alpha}}{(1 - 2\cos \varepsilon e^{-\alpha} + e^{-2\alpha})^{3/2}}.$$

Taking the limit $\alpha \rightarrow 0^+$ on both sides we find

$$\lim_{\alpha \rightarrow 0^+} \sum_{l=0}^{\infty} (2l+1) P_l(\cos \varepsilon) e^{-\alpha l} = 0. \quad (\text{B3})$$

But this is exactly the definition of the generalized sum in Eq. (B1). Q.E.D.

Next, we want to prove that

$$\sum_{l=0}^{\infty} (2l+1) [l(l+1)]^n P_l(\cos \varepsilon) = 0,$$

for every $n \in \mathbb{N}$. This is easily done by induction, first assuming that for some $n = k$

$$\sum_{l=0}^{\infty} (2l+1) [l(l+1)]^k P_l(\cos \varepsilon) = 0,$$

and proving the equality holds for $n = k+1$ as well — since we already know it is true for $n = 0$. The differential equation that defines the Legendre polynomials can be written (see Ref. [13]) in the form

$$l(l+1) P_l(\cos \varepsilon) = -\sin^2 \varepsilon \frac{\partial^2 P_l(\cos \varepsilon)}{(\partial \cos \varepsilon)^2} + 2 \cos \varepsilon \frac{\partial P_l(\cos \varepsilon)}{\partial \cos \varepsilon},$$

hence

$$\begin{aligned} & \sum_{l=0}^{\infty} (2l+1) [l(l+1)]^{k+1} P_l(\cos \varepsilon) \\ &= \sum_{l=0}^{\infty} (2l+1) [l(l+1)]^k \left[-\sin^2 \varepsilon \frac{\partial^2 P_l(\cos \varepsilon)}{(\partial \cos \varepsilon)^2} + 2 \cos \varepsilon \frac{\partial P_l(\cos \varepsilon)}{\partial \cos \varepsilon} \right] = \\ &= \left[-\sin^2 \varepsilon \frac{\partial^2}{(\partial \cos \varepsilon)^2} + 2 \cos \varepsilon \frac{\partial}{\partial \cos \varepsilon} \right] \sum_{l=0}^{\infty} (2l+1) [l(l+1)]^k P_l(\cos \varepsilon) = 0. \end{aligned}$$

Q.E.D.

Appendix C: Legendre decomposition of the counter-term

This Appendix deals with the Legendre decomposition of the counter-term as given in Eq. (3.10). Namely, we obtain the decompositions (3.16) and (3.17) for the functions $\sin^{-2}(\varepsilon/2)$ and $\ln[\sin(\varepsilon/2)]$ respectively.

First we treat the term $\sin^{-2}(\varepsilon/2)$, and to this end we define

$$S(\alpha) \equiv \sum_{l=0}^{\infty} \frac{2l+1}{2} h(l) P_l(z) e^{-\alpha l} = \sum_{l=1}^{\infty} \frac{2l+1}{2} h(l) P_l(z) e^{-\alpha l}, \quad (\text{C1})$$

where $h(l)$ is the harmonic number. [Here and throughout this Appendix all sums are conventional ones, except in Eq. (C6).] Using the Legendre identity [13]

$$(2l+1)zP_l(z) = (l+1)P_{l+1}(z) + lP_{l-1}(z),$$

one can write $2zS(\alpha)$ as

$$2zS(\alpha) = \sum_{l=1}^{\infty} h(l)(l+1)P_{l+1}(z)e^{-\alpha l} + \sum_{l=1}^{\infty} h(l)lP_{l-1}(z)e^{-\alpha l}.$$

Renaming the l index so as to retain P_l (rather than $P_{l\pm 1}$) in both sums, we obtain

$$2zS(\alpha) = e^{\alpha} \sum_{l=2}^{\infty} h(l-1)lP_l(z)e^{-\alpha l} + e^{-\alpha} \sum_{l=0}^{\infty} h(l+1)(l+1)P_l(z)e^{-\alpha l}.$$

However, we want to start the summation at $l=1$ (instead of 2 or 0) in both sums. In the first sum this change is free because $h(0)=0$, but in the second sum we must compensate it by adding the $l=0$ contribution which amounts to $e^{-\alpha}$:

$$2zS(\alpha) = e^{\alpha} \sum_{l=1}^{\infty} h(l-1)lP_l(z)e^{-\alpha l} + e^{-\alpha} \sum_{l=1}^{\infty} h(l+1)(l+1)P_l(z)e^{-\alpha l} + e^{-\alpha}.$$

We now re-express the two sums in terms of $h(l)$ rather than $h(l\pm 1)$:

$$2zS(\alpha) = e^{\alpha} \sum_{l=1}^{\infty} \left[h(l) - \frac{1}{l} \right] lP_l(z)e^{-\alpha l} + e^{-\alpha} \sum_{l=1}^{\infty} \left[h(l) + \frac{1}{l+1} \right] (l+1)P_l(z)e^{-\alpha l} + e^{-\alpha},$$

which we recast as

$$2zS(\alpha) = \sum_{l=1}^{\infty} h(l) [le^{\alpha} + (l+1)e^{-\alpha}] P_l(z)e^{-\alpha l} - 2\sinh(\alpha) \sum_{l=1}^{\infty} P_l(z)e^{-\alpha l} + e^{-\alpha}. \quad (\text{C2})$$

Let us elaborate on the first sum in Eq. (C2). We write it in the form

$$\sum_{l=1}^{\infty} h(l) [(2l+1)\cosh(\alpha) - \sinh(\alpha)] P_l(z)e^{-\alpha l},$$

and using the definition of $S(\alpha)$ we re-express this sum as

$$2\cosh(\alpha)S(\alpha) - \sinh(\alpha) \sum_{l=1}^{\infty} h(l) P_l(z)e^{-\alpha l}. \quad (\text{C3})$$

The second sum in Eq. (C2) can be directly computed (for $|z| < 1$ and $\alpha > 0$) by setting $\cos \varepsilon = z$ and $t = e^{-\alpha}$ in the generating function (B2):

$$\sum_{l=1}^{\infty} P_l(z) e^{-\alpha l} = \frac{1}{\sqrt{1 - 2ze^{-\alpha} + e^{-2\alpha}}} - 1 .$$

Substituting this back in Eq. (C2), along with the expression (C3) for the first sum, we obtain

$$2zS(\alpha) = 2 \cosh(\alpha)S(\alpha) - \sinh(\alpha) \sum_{l=1}^{\infty} h(l) P_l(z) e^{-\alpha l} + e^{\alpha} - \frac{2 \sinh(\alpha)}{\sqrt{1 - 2ze^{-\alpha} + e^{-2\alpha}}} . \quad (C4)$$

Consider now the limit $\alpha \rightarrow 0^+$ of this equation. The last term vanishes (recall that we consider here $z < 1$). Concerning the term $\propto \sinh(\alpha)$, we assume here that the sum over l does not diverge as $\alpha \rightarrow 0^+$, hence this term vanishes too.¹⁹ Applying this limit to both sides of the equation we now obtain

$$2z \lim_{\alpha \rightarrow 0^+} S(\alpha) = 2 \lim_{\alpha \rightarrow 0^+} S(\alpha) + 1 .$$

Setting $z = \cos \varepsilon$ and extracting the desired limit of $S(\alpha)$ we find

$$\lim_{\alpha \rightarrow 0^+} S(\alpha) = \frac{1}{2(z-1)} = -\frac{1}{2(1-\cos \varepsilon)} = -\frac{1}{4 \sin^2(\varepsilon/2)} . \quad (C5)$$

Recalling Eq. (C1), we finally obtain

$$\sum_{l=0}^{\infty} \frac{2l+1}{2} h(l) P_l(\cos \varepsilon) = -\frac{1}{4 \sin^2(\varepsilon/2)} \quad (C6)$$

(this time with a *generalized* sum), thereby recovering Eq. (3.16). Q.E.D.

The second Legendre decomposition needed for the counter-term is that of $\ln[\sin(\varepsilon/2)]$. Expressing it in the form

$$\ln[\sin(\varepsilon/2)] = \sum_{l=0}^{\infty} \frac{2l+1}{2} \Lambda(l) P_l(\cos \varepsilon)$$

(in accord with Eq. (3.17)), we need to calculate the expansion coefficients $\Lambda(l)$. We define $z = \cos \varepsilon$, and noting that

$$\ln[\sin(\varepsilon/2)] = \frac{1}{2} \ln\left(\frac{1-z}{2}\right) ,$$

the desired coefficients are given by the Legendre integral

$$\Lambda(l) = \int_{-1}^1 \frac{1}{2} \ln\left(\frac{1-z}{2}\right) P_l(z) dz .$$

¹⁹ It is actually possible to proceed without using this non-divergence assumption: Denoting the sum in Eq. (C4) by $\tilde{S}(\alpha)$, notice that $S = \tilde{S}/2 - d\tilde{S}/d\alpha$, which allows one to treat Eq. (C4) as a linear ODE for $\tilde{S}(\alpha)$. This ODE is solvable, yielding an explicit expression for $\tilde{S}(\alpha)$ and hence $S(\alpha)$. We shall not display this expression here as it is too long. Nevertheless, when the limit $\alpha \rightarrow 0^+$ is taken, we recover Eq. (C5).

For $l = 0$ this integral is trivial and the result is $\Lambda(0) = -1$. For $l > 0$ one can use the Legendre equation to rewrite it as

$$\Lambda(l) = -\frac{1}{2l(l+1)} \int_{-1}^1 \ln\left(\frac{1-z}{2}\right) \frac{d}{dz} \left[(1-z^2) \frac{d}{dz} P_l(z) \right] dz.$$

Integrating by parts yields

$$\Lambda(l) = -\frac{1}{2l(l+1)} \int_{-1}^1 (1+z) \frac{d}{dz} P_l(z) dz,$$

as the boundary term vanishes. Integrating by parts once again gives

$$\Lambda(l) = -\frac{1}{2l(l+1)} \left[[(1+z) P_l(z)]_{-1}^1 - \int_{-1}^1 P_l(z) dz \right].$$

The integral vanishes for all $l > 0$, and from the $z = 1$ limit of the first term we are left with

$$\Lambda(l) = -\frac{1}{l(l+1)}.$$

We conclude that

$$\Lambda(l) = \begin{cases} -1 & l = 0 \\ -\frac{1}{l(l+1)} & l > 0 \end{cases}.$$

Q.E.D.

Appendix D: Large- ω expansion

In this Appendix we explore the asymptotic behavior of the field modes $\psi_{\omega l}$ at large ω . More specifically, we expand these quantities in powers of $1/\omega$ (at fixed l). Understanding this large- ω asymptotic behavior is necessary in angular splitting because the integral of $|\bar{\psi}_{\omega l}|^2$ (which is $\propto |\psi_{\omega l}|^2/\omega$) over ω diverges; and in order to regularize it we need to subtract the appropriate large- ω piece.

Luckily, the regularization of $\langle \phi^2 \rangle$ only requires the leading-order term in the expansion (namely the term $\propto \omega^0$ in ψ).²⁰ A crucial outcome of the expansion below is that this leading-order term is independent of l . This allows us to regularize the ω -integral by simply subtracting the $l = 0$ contribution (see Sec. III A 1).

But the large- ω expansion has an additional purpose: Even after the leading term in $|\bar{\psi}_{\omega l}|^2$ has been subtracted, the integral of the remaining piece decays rather slowly, typically like ω^{-2} . In principle we need to integrate up to $\omega = \infty$, but in practice we can only carry the numerical integration up to some finite value ω_{max} . To account for the missing contribution from $\omega > \omega_{max}$, we replace the integrand in this large- ω domain by its power series in $1/\omega$, up to a sufficient order. For example, in the numerical implementation in the Schwarzschild case we use the terms up to order ω^{-8} (see Sec. IV A). The reminder decays very rapidly, hence its contribution at $\omega > \omega_{max}$ is negligible.

²⁰ For the calculation of the renormalized stress-energy tensor one need to subtract terms up to order ω^{-2} .

The large- ω expansion looks different in the eternal and regular-center cases (also in each of these cases there are differences between static and time-dependent backgrounds). The eternal case is simpler, because there are no reflections in the large- ω limit. On the other hand, in the presence of a regular center waves are fully reflected off the origin, even for arbitrarily large ω . Owing to interference of the propagating and reflected pieces, $|\bar{\psi}_{\omega l}|^2$ turns out to be oscillatory in the regular-center case, in contrast to its monotonic behavior in the eternal case. This makes the large- ω expansion more complicated in the case of regular center. (And in both cases, the time-dependent problem is obviously more complicated than the static one.)

In what follows we shall describe the analysis in some detail in the simplest case of static eternal background. This is also the case that we need to support our numerical analysis in Schwarzschild. We shall provide here the expansion coefficients up to order ω^{-8} . The analysis of the three other cases is more lengthy, and we hope to present it elsewhere. Nevertheless, in the last subsection we shall summarize the final results in all four cases (namely eternal and regular center; static and time-dependent), concerning the leading order term — the term needed for regularizing the integral over ω .

1. Static eternal BH background

In an eternal background, for each ω and l there are two sets of basis solutions $\psi_{\omega l}^{in}$ and $\psi_{\omega l}^{up}$, both satisfy the same radial equation (3.3). Let ψ stand for either $\psi_{\omega l}^{in}$ or $\psi_{\omega l}^{up}$. We express its large- ω asymptotic behavior as

$$\psi(z) = e^{\pm i\omega z} \sum_{k=0}^{\infty} \frac{a_k(z)}{\omega^k} + [\dots], \quad (\text{D1})$$

where “[...]” denotes possible terms that decay faster than any power of $1/\omega$. Inserting Eq. (D1) in the radial equation we obtain a simple recursion relation

$$\pm 2ia'_{k+1} = -a''_k + V_l a_k.$$

When applying this expansion to $\psi_{\omega l}^{in}$ and $\psi_{\omega l}^{up}$, we denote the corresponding coefficients by a_k^{in} and a_k^{up} . We now need to use the appropriate boundary conditions at the horizon and infinity. These are given by Eq. (3.27) wherein, in the large- ω domain, we may set the coefficient $\rho \rightarrow 0$ (recalling that the reflection coefficient ρ decays faster than any power of $1/\omega$). This matching tells us at once that (i) $\psi_{\omega l}^{in}$ and $\psi_{\omega l}^{up}$ are respectively associated with the “-” and “+” signs in Eq. (D1); (ii) In both of them the leading-order term is $a_0^{in} = a_0^{up} = 1$, and (iii) for all $k > 0$, a_k^{in} vanishes at $z \rightarrow \infty$ and a_k^{up} at $z \rightarrow -\infty$. We thus obtain the integrated recursion relations for a_k^{in} and a_k^{up} :

$$\begin{aligned} a_{k+1}^{in} &= -\frac{i}{2} (a_k^{in})' + \frac{i}{2} \int_{\infty}^z V_l a_k^{in} d\bar{z}, \\ a_{k+1}^{up} &= \frac{i}{2} (a_k^{up})' - \frac{i}{2} \int_{-\infty}^z V_l a_k^{up} d\bar{z}. \end{aligned}$$

The calculation of a_k^{in} and a_k^{up} is now straightforward, for any k . Note that the coefficients $a_k^{in,up}$ depend on the functional form of $V_l(z)$, usually in a (multi-) integral manner.

Next we calculate the large- ω asymptotic behavior of $|\psi_{\omega l}^{in}|^2$ and $|\psi_{\omega l}^{up}|^2$, which we express as

$$|\psi(z)|^2 = \sum_{k=0}^{\infty} \frac{b_k(z)}{\omega^k} + [\dots],$$

again using the generic symbol ψ for either $\psi_{\omega l}^{in}$ or $\psi_{\omega l}^{up}$. After executing all the z -integrals, the resulting coefficients $b_k(z)$ (namely b_k^{in} and b_k^{up}) turn out to be rather simple, and they demonstrate several surprising features: (i) b_k *vanish* for all odd k ; (ii) for all even k , $b_k(z)$ depends on $V_l(z)$ in a *direct, local manner* [in contrast with the non-local, integral character of the more elementary coefficients $a_k^{in,up}(z)$]; (iii) The coefficients $b_k^{in}(z)$ and $b_k^{up}(z)$ are *exactly the same*, for any k . (The derivation of these properties (i-iii) is interesting, but is way beyond the scope of the present paper.) We may therefore write the large- ω expansion in the form

$$|\psi_{\omega l}^{in}(z)|^2 = |\psi_{\omega l}^{up}(z)|^2 = \sum_{k=0}^{\infty} \frac{b_{2k}(z)}{\omega^{2k}} + [\dots]. \quad (\text{D2})$$

We give here the explicit form of the first few b_{2k} coefficients:

$$b_0 = 1, \quad b_2 = \frac{V_l}{2}, \quad b_4 = \frac{1}{8} (3V_l^2 - V_l''), \quad b_6 = \frac{1}{32} (V_l^{(4)} - 10V_l V_l'' - 5V_l'^2 + 10V_l^3), \quad (\text{D3})$$

$$b_8 = \frac{1}{128} [35V_l^4 - 70V_l^2 V_l'' + 21V_l''^2 + 14V_l (V_l^{(4)} - 5V_l'^2) + 28V_l^{(3)} V_l' - V_l^{(6)}], \quad (\text{D4})$$

where a superscript (n) denotes $(\partial/\partial z)^n$.

We used these coefficients in the Schwarzschild and RN cases, for handling the large- ω domain in the numerical integration of $|\bar{\psi}_{\omega l}|^2$. In turn, this numerical calculation confirmed the validity of the expansion (D2) along with the coefficients (D3,D4) (so far in the Schwarzschild and RN cases).

Finally, recalling the relation (3.2) between $\psi_{\omega l}$ and $\bar{\psi}_{\omega l}$, we conclude that at leading order both $|\bar{\psi}_{\omega l}^{in}(z)|^2$ and $|\bar{\psi}_{\omega l}^{up}(z)|^2$ are equal to $1/(4\pi r^2 \omega)$ (and are hence independent of l), with corrections $\propto \omega^{-3}$.

2. Leading order: summary of results

We summarize here (without proof) the main results concerning the leading-order behavior of $|\bar{\Psi}_{\omega l}(z)|$ in the large- ω expansion. These results include the eternal and non-eternal cases, for both static and time-dependent backgrounds.

Recall that in the static case $\bar{\psi}_{\omega l}$ differs from $\bar{\Psi}_{\omega l}$ by the factor $e^{-i\omega t}$ only, therefore $|\bar{\Psi}_{\omega l}| = |\bar{\psi}_{\omega l}|$.

a. Eternal BH

In this case we obtain

$$|\bar{\Psi}_{\omega l}^{in}(t, z)|^2 = |\bar{\Psi}_{\omega l}^{up}(t, z)|^2 = \frac{1}{4\pi r^2 \omega} + O(\omega^{-3}). \quad (\text{D5})$$

We already derived this result in the previous subsection for the static case, but this relation holds in the time-dependent case as well.

b. Regular center

In this case there is only one mode function $\bar{\Psi}_{\omega l}(t, z)$ for each ω and l . Its large- ω asymptotic behavior is found to be

$$|\bar{\Psi}_{\omega l}(t, z)|^2 = \frac{1}{2\pi r^2 \omega} + (\dots), \quad (\text{D6})$$

where “(…)” denotes terms whose integral over ω converges. These include two types of terms: (i) terms which decay faster than $1/\omega$, and (ii) oscillatory terms whose amplitude decays as $1/\omega$ (or faster), and are hence integrable.

In the static case we can show that the terms of type (i) (the non-oscillatory terms) decay as ω^{-3} . In the time-dependent case we haven’t yet obtained the specific decay power of this subdominant term, we can only show it is faster than $1/\omega$.

A simple interesting example is the Minkowski background (namely $\Gamma = 1$, $r = z$): In this case the exact solution for $\psi_{\omega l}(r)$ is

$$\psi_{\omega l}(r) = \sqrt{2\pi\omega r} J_{l+1/2}(\omega r)$$

where J denotes the Bessel function of the first kind. The asymptotic behavior at large ω (for fixed $r > 0$) is

$$|\psi_{\omega l}(r)|^2 = 4 \sin^2(\omega r - l\pi/2) + O(\omega^{-1}), \quad (\text{D7})$$

which yields

$$|\bar{\Psi}_{\omega l}(r)|^2 = |\bar{\psi}_{\omega l}(r)|^2 = \frac{1}{2\pi r^2 \omega} + \frac{(-1)^{l+1}}{2\pi r^2 \omega} \cos(2r\omega) + O(\omega^{-2}), \quad (\text{D8})$$

in agreement with Eq. (D6).

-
- [1] S. W. Hawking, Commun. Math. Phys. **43**,199 (1975).
 - [2] B. S. DeWitt, Dynamical Theory of Groups and Fields (Gordon and Breach, New York, 1965).
 - [3] S. M. Christensen, Phys. Rev. D **14**, 2490 (1976).
 - [4] P. Candelas and K. W. Howard, Phys. Rev. D **29**, 1618 (1984).
 - [5] K. W. Howard, Phys. Rev. D **30**, 2532 (1984).
 - [6] P. R. Anderson, Phys. Rev. D **41**, 1152 (1990).
 - [7] P. R. Anderson, W. A. Hiscock, D. A. Samuel, Phys. Rev. D **51**, 4337 (1995).
 - [8] See also a more recent analysis in Kerr background: G. Duffy and A. C. Ottewill, Phys. Rev. D **77**, 024007 (2008). They analyzed the renormalized stress-energy tensor in a portion of a Kerr BH, in a “Hartle-Hawking like” state, by imposing nonphysical boundary conditions using a mirror.
 - [9] T.S. Bunch and P. C. W. Davies, Proc. R. Soc. Lond. A **357** 381-394 (1977).
 - [10] A. Levi, A. Ori, Phys. Rev. D **91**, 104028 (2015).
 - [11] S. M. Christensen and S. A. Fulling, Phys. Rev. D **15**, 2088 (1977).
 - [12] P. Candelas, Phys. Rev. D **21**, 2185 (1980).
 - [13] G. B. Arfken and H. J. Weber, Mathematical Methods for Physicists, 5th edition, (Academic Press, San Diego, 2001).

- [14] M. Abramowitz and I. A. Stegun, Handbook of Mathematical Functions, 10th edition, (National Bureau of Standards, Washington, 1972).
- [15] P. Anderson, private communication.
- [16] B. S. Kay and R. M. Wald, Phys. Reps. 207 49 (1991).
- [17] A. C. Ottewill and E. Winstanley, Phys. Rev. D **62**, 084018 (2000).